

*Helen: File under SR-25
(Miss Colburn, F. G.)*

*JH
&
TFM*

FINAL REPORT

ON

**APPLICATION OF THE EXPLOSIVE TEST TO EVALUATE SHOCK
PROPERTIES OF HIGH YIELD STRENGTH STEELS**

**PART I - PRELIMINARY INVESTIGATION OF TECHNIQUES FOR
DIRECT EXPLOSION TESTING OF HIGH YIELD
STRENGTH STEELS**

BY

A. MULLER, W. G. BENZ and W. A. SNELLING

**PART II - THEORETICAL INVESTIGATION OF THE FRACTURE
OF STEEL PLATES UNDER EXPLOSIVE LOADING**

BY

EDWARD SAIBEL

**Air Reduction Company, Inc.
Under Bureau of Ships Contract NObs-34232**

COMMITTEE ON SHIP CONSTRUCTION

DIVISION OF ENGINEERING AND INDUSTRIAL RESEARCH

NATIONAL RESEARCH COUNCIL

ADVISORY TO

SHIP STRUCTURE COMMITTEE

UNDER

**Bureau of Ships, Navy Department
Contract NObs-34231**

SERIAL NO. SSC-29

COPY NO. 26

DATE: JULY 13, 1949

Code 343

NAVY DEPARTMENT

NObs-34323 (343)

Bureau of Ships

Washington 25, D. C.

AUG 10 1949

Lt. Comdr. James McIntosh
U. S. Coast Guard Headquarters
1300 E Street, N. W.
Washington 25, D. C.

Dear Sir:

SUBJECT: Final Report on "Application of the Explosion Test to
Evaluate Shock Properties of High Yield Strength Steels"
SSC-29, Air Reduction Company, Inc., Murray Hill, N. J.
Contract NObs-34232.

There is enclosed for your information and file one copy of the
subject report as follows:

<u>Report Serial No.</u>	<u>Date</u>	<u>Copy No.</u>
SSC-29	July 13, 1949	-----26

Any comments on this report which you care to submit will be appre-
ciated and should be addressed to the Chief, Bureau of Ships,
attention Code 343:

Sincerely yours,

C. M. Tooke

C. M. TOOKE
By direction of
Chief of Bureau

Encl.

NATIONAL RESEARCH COUNCIL
2101 CONSTITUTION AVENUE, WASHINGTON, D. C.

Established in 1916 by the National Academy of Sciences under its Congressional
Charter and organized with the cooperation of the National Scientific
and Technical Societies of the United States

DIVISION OF ENGINEERING AND INDUSTRIAL RESEARCH

July 13, 1949

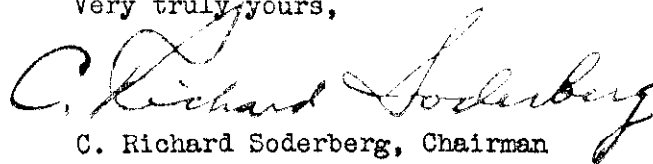
Chief, Bureau of Ships
Code 343
Navy Department
Washington 25, D.C.

Dear Sir:

Attached is Report Serial No. SSC-29 entitled
"Application of the Explosive Test to Evaluate Shock Properties
of High Yield Strength Steels." This report has been sub-
mitted by the contractor as a Final Report of the work done
on Research Project SR-25 under Contract NObs-34232 between
the Bureau of Ships, Navy Department and the Air Reduction
Company, Inc.

The report has been reviewed and acceptance recom-
mended by representatives of the Committee on Ship Con-
struction, Division of Engineering and Industrial Research,
NRC, in accordance with the terms of the contract between
the Bureau of Ships, Navy Department and the National Academy
of Sciences.

Very truly yours,



C. Richard Soderberg, Chairman
Division of Engineering and
Industrial Research

GRS:mh
Enclosure

PREFACE

The Navy Department through the Bureau of Ships is distributing this report to those agencies and individuals who were actively associated with the research work. This report represents a part of the research work contracted for under the section of the Navy's directive "to investigate the design and construction of welded steel merchant vessels."

The distribution of this report is as follows:

Copy No. 1 - Chief, Bureau of Ships, Navy Department
Copy No. 2 - Dr. D.W. Bronk, Chairman, National Research Council

Committee on Ship Construction

Copy No. 3 - V. H. Schnee, Chairman
Copy No. 4 - J. L. Bates
Copy No. 5 - H. C. Boardman
Copy No. 6 - Paul Ffield
Copy No. 7 - M. A. Grossman
Copy No. 8 - C. H. Herty, Jr.
Copy No. 9 - A. B. Kinzel
Copy No. 10 - J. M. Lessells
Copy No. 11 - G. S. Mikhalapov
Copy No. 12 - J. Ormondroyd
Copy No. 13 - H. W. Pierce
Copy No. 14 - E. C. Smith
Copy No. 15 - T. T. Watson
Copy No. 16 - Finn Jonassen, Research Coordinator

Members of Project Advisory Committees SR-25, SR-92,
SR-96, SR-98, SR-99, SR-100 and SR-101

Copy No. 16 - Finn Jonassen, Chairman
Copy No. 17 - R.H. Aborn
Copy No. 18 - L. C. Bibber
Copy No. 5 - H. C. Boardman
Copy No. 19 - T. J. Dolan
Copy No. 6 - Paul Ffield
Copy No. 7 - M. A. Grossman
Copy No. 8 - C. H. Herty, Jr.
Copy No. 20 - C. E. Jackson
Copy No. 10 - J. M. Lessells
Copy No. 21 - M. W. Lightner
Copy No. 11 - G. S. Mikhalapov
Copy No. 12 - J. Ormondroyd
Copy No. 22 - R. E. Peterson
Copy No. 13 - H. W. Pierce
Copy No. 23 - R. L. Rickett
Copy No. 14 - E. C. Smith
Copy No. 15 - T. T. Watson
Copy No. 24 - A. G. Bissell, Bureau of Ships, Liaison
Copy No. 25 - Mathew Letich, American Bureau of Shipping, Liaison
Copy No. 26 - James McIntosh, U.S. Coast Guard, Liaison

Copy No. 27 - Comdr. R. D. Schmidtman, U. S. Coast Guard, Liaison
Copy No. 28 - T. L. Soo-Hoo, Bureau of Ships, Liaison
Copy No. 29 - Wm. Spraragen, Welding Research Council, Liaison
Copy No. 30 - R. E. Wiley, Bureau of Ships, Liaison
Copy No. 31 - J. L. Wilson, American Bureau of Shipping, Liaison

Ship Structure Committee

Copy No. 32 - Rear Admiral Ellis Reed-Hill, USCG - Chairman
Copy No. 33 - Rear Admiral Charles D. Wheelock, USN, Bureau of Ships
Copy No. 34 - Brigadier Gen. Paul F. Yount, War Department
Copy No. 35 - Captain J. L. McGuigan, U. S. Maritime Commission
Copy No. 36 - D. P. Brown, American Bureau of Shipping
Copy No. 3 - V. H. Schnee, Committee on Ship Construction - Liaison

Ship Structure Subcommittee

Copy No. 37 - Captain C. M. Tooke, USN, Bureau of Ships, Chairman
Copy No. 38 - Captain R. A. Hinners, USN, David Taylor Model Basin
Copy No. 39 - Comdr. R. H. Lambert, USN, Bureau of Ships
Copy No. 27 - Comdr. R. D. Schmidtman, USCG, U. S. Coast Guard Headquarters
Copy No. 40 - W. G. Frederick, U. S. Maritime Commission
Copy No. 41 - Hubert Kempel, Office, Chief of Transportation, War Department
Copy No. 25 - Mathew Letich, American Bureau of Shipping
Copy No. 26 - James McIntosh, U. S. Coast Guard
Copy No. 42 - R. M. Robertson, Office of Naval Research, U. S. Navy
Copy No. 43 - V. L. Russo, U. S. Maritime Commission
Copy No. 30 - R. E. Wiley, Bureau of Ships, U. S. Navy
Copy No. 31 - J. L. Wilson, American Bureau of Shipping
Copy No. 16 - Finn Jonassen, Liaison Representative, NRC
Copy No. 44 - E. H. Davidson, Liaison Representative, AISI
Copy No. 45 - W. Paul Gerhart, Liaison Representative, AISI
Copy No. 29 - Wm. Spraragen, Liaison Representative, WRC

Navy Department

Copy No. 46 - Comdr. R. S. Mandelkorn, USN, Armed Forces Special Weapons Project
Copy No. 24 - A. G. Bissell, Bureau of Ships
Copy No. 47 - A. Amirikian, Bureau of Yards and Docks
Copy No. 48 - J. W. Jenkins, Bureau of Ships
Copy No. 49 - Noah Kahn, New York Naval Shipyard
Copy No. 50 - E. M. MacCutcheon, Jr., David Taylor Model Basin
Copy No. 51 - W. R. Osgood, David Taylor Model Basin
Copy No. 52 - M. E. Promisel, Bureau of Aeronautics
Copy No. 53 - John Vasta, Bureau of Ships
Copy No. 54 - J. E. Walker, Bureau of Ships
Copies 55 and 56 - U. S. Naval Engineering Experiment Station
Copy No. 57 - U. S. Naval Gun Factory, Attn. Code IN910
Copy No. 58 - U. S. Naval Proving Ground, Attn. Armor & Projectile Lab.
Copy No. 59 - Bureau of Ordnance, Attn. Re3
Copy No. 60 - Naval Research Laboratory, Attn. Mechanics Div., Code 3800
Copy No. 61 - New York Naval Shipyard, Material Laboratory
Copy No. 62 - Industrial Testing Laboratory, Philadelphia Naval Shipyard

Copy No. 63 - Philadelphia Naval Shipyard
Copy No. 64 - San Francisco Naval Shipyard
Copy No. 65 - David Taylor Model Basin, Attn. Library
Copies 66 and 67 - Publications Board, Navy Dept. via Bureau of Ships, Code 330c
Copies 68 and 69 - Technical Library, Bureau of Ships, Code 337-L

U. S. Coast Guard

Copy No. 70 - Captain R. B. Lank, Jr., USCG
Copy No. 71 - Captain G. A. Tyler, USCG
Copy No. 72 - Testing and Development Division
Copy No. 73 - U. S. Coast Guard Academy, New London

U. S. Maritime Commission

Copy No. 74 - E. E. Martinsky

Representatives of American Iron and Steel Institute
Committee on Manufacturing Problems

Copy No. 75 - C. M. Parker, Secretary, General Technical Committee,
American Iron and Steel Institute
Copy No. 18 - L. C. Bibber, Carnegie-Illinois Steel Corp.
Copy No. 8 - C. H. Herty, Jr., Bethlehem Steel Company
Copy No. 14 - E. C. Smith, Republic Steel Company

Welding Research Council

Copy No. 76 - C. A. Adams
Copy No. 77 - Everett Chapman
Copy No. 78 - LaMotte Grover
Copy No. 29 - Wm. Spraragen

Committee on Ship Steel

Copy No. 79 - R. F. Mehl, Chairman
Copy No. 8 - C. H. Herty, Jr., Vice Chairman
Copy No. 80 - Wm. M. Baldwin, Jr.
Copy No. 81 - Chas. S. Barrett
Copy No. 82 - R. M. Brick
Copy No. 83 - S. L. Hoyt
Copy No. 84 - I. R. Kramer
Copy No. 21 - M. W. Lightner
Copy No. 85 - T. S. Washburn
Copy No. 16 - Finn Jonassen, Technical Director
Copy No. 86 - R. H. Raring, Technical Secretary

Copy No. 87 - C. R. Soderberg, Chairman, Div. Eng. & Ind. Research, NRC
Copy No. 3 - V. H. Schnee, Chairman, Committee on Ship Construction
Copy No. 16 - Finn Jonassen, Research Coordinator, Committee on Ship Construction
Copy No. 88 - A. Muller, Investigator, Research Project SR-25
Copy No. 89 - W. G. Benz, Investigator, Research Project SR-25
Copy No. 90 - W. A. Snelling, Investigator, Research Project SR-25
Copy No. 91 - E. Saibel, Investigator, Research Project SR-25

Copy No. 92 - S. T. Carpenter, Investigator, Research Project SR-98
 Copy No. 93 - L. J. Ebert, Investigator, Research Project SR-99
 Copy No. 10 - J. M. Lessells, Investigator, Research Project SR-101
 Copy No. 94 - C. W. MacGregor, Investigator, Research Project SR-102
 Copy No. 95 - C. E. Sims, Investigator, Research Project SR-110
 Copy No. 96 - E. W. Suppiger, Investigator, Research Project SR-113
 Copy No. 97 - C. B. Voldrich, Investigator, Research Project SR-100
 Copy No. 98 - Clarence Altenburger, Great Lakes Steel Company
 Copy No. 99 - J. G. Althouse, Lukens Steel Company
 Copy No. 100 - A. B. Bagsar, Sun Oil Company
 Copy No. 101 - British Shipbuilding Research Assn., Attn: J. C. Asher, Sec.
 Copy No. 102 - E. L. Cochran, Massachusetts Institute of Technology
 Copy No. 103 - George Ellinger, National Bureau of Standards
 Copy No. 104 - M. Gensamer, Carnegie-Illinois Steel Corp.
 Copy No. 105 - M. F. Hawkes, Carnegie Institute of Technology
 Copy No. 106 - W. F. Hess, Rensselaer Polytechnic Institute
 Copy No. 107 - O. J. Horger, Timken Roller Bearing Company
 Copy No. 108 - Bruce Johnston, Fritz Laboratory, Lehigh University
 Copy No. 109 - P. E. Kyle, Cornell University
 Copy No. 110 - J. R. Low, Jr., General Electric Company
 Copy No. 111 - N. M. Fewmark, University of Illinois
 Copy No. 112 - J. T. Norton, Massachusetts Institute of Technology
 Copy No. 113 - Ordnance Department, Armor Section, Attn. Col. A. P. Taber
 Copy No. 114 - Ordnance Research & Development, Attn. ORDTB - Materials
 Copy No. 115 - W. A. Reich, General Electric Company
 Copy No. 116 - L. J. Rohl, Carnegie-Illinois Steel Corp.
 Copy No. 117 - W. P. Roop, Swarthmore College
 Copy No. 118 - R. D. Stout, Lehigh University
 Copy No. 119 - Saylor Snyder, Carnegie-Illinois Steel Corp.
 Copy No. 120 - Watertown Arsenal Laboratory, Attn. J. F. Wallace
 Copies 121 thru 145 - Sir Chas. Wright, British Joint Services Mission(Navy Staff)
 Copy No. 146 - Carl A. Zapffe, Carl A. Zapffe Laboratories
 Copy No. 147 - International Nickel Co., Inc., Attn. T. N. Armstrong
 Copy No. 148 - Transportation Corps Board, Brooklyn, N. Y.
 Copies 149 thru 153 - Library of Congress via Bureau of Ships, Code 330c
 Copy No. 154 - File Copy, Committee on Ship Steel
 Copy No. 155 - NACA, Attn. Materials Research Coordination, U. S. Navy
 Copies 156 thru 160 - Bureau of Ships, Code 343

Copy No. 161 -
 Copy No. 162 -
 Copy No. 163 -
 Copy No. 164 -
 Copy No. 165 -
 Copy No. 166 -
 Copy No. 167 -
 Copy No. 168 -
 Copy No. 169 -
 Copy No. 170 -
 Copy No. 171 -
 Copy No. 172 -
 Copy No. 173 -
 Copy No. 174 -
 Copy No. 175 -

(Total - 175 copies)

FINAL REPORT

of

APPLICATION OF THE EXPLOSION TEST TO EVALUATE
SHOCK PROPERTIES OF HIGH YIELD STRENGTH STEELS

PART I

PRELIMINARY INVESTIGATION OF TECHNIQUES FOR DIRECT
EXPLOSION TESTING OF HIGH YIELD STRENGTH STEELS

by

A. Muller, W. G. Benz, and W. A. Snelling

PART II

THEORETICAL INVESTIGATION OF THE FRACTURE OF
STEEL PLATES UNDER EXPLOSIVE LOADING

by

Edward Saibel

BUREAU OF SHIPS, NAVY DEPARTMENT
Contract NObs-34232

AIR REDUCTION LABORATORIES
AIR REDUCTION COMPANY, INC.
MURRAY HILL, NEW JERSEY

PART I

PRELIMINARY INVESTIGATION OF TECHNIQUES FOR DIRECT
EXPLOSION TESTING OF HIGH YIELD STRENGTH STEELS

ABSTRACT

Results of a preliminary investigation to establish optimum technique for direct-explosion testing of high yield strength steels has been undertaken. Optimum test-plate size, method of supporting test plate, and type of explosive required have been established.

A theoretical study of the state of stress existing in test plates was made.

TABLE OF CONTENTS

	<u>Page</u>
ABSTRACT	i
LIST OF TABLES	ii
LIST OF FIGURES	iii
GLOSSARY	iv
SUMMARY	1
INTRODUCTION	3
DETAILS OF THE DIRECT-EXPLOSION TEST	7
MATERIAL	10
RESULTS OF DIRECT-EXPLOSION TEST	13
BIBLIOGRAPHY	17
APPENDIX A	
Preliminary Investigation of Influence of Size of Test Plate on Shock Limit of One-inch Low-Alloy NI-CR Steel	A-1
APPENDIX B	
Determination of Detonation Velocity of Explosives	B-1
APPENDIX C	
Comparison of Efficacy of Platen Quenching and Brine Quenching after Austenitizing of Low-Alloy MN-MO Steel	C-1

LIST OF TABLES

		<u>Page</u>
TABLE I	V-Notch Charpy Impact Strength of One-Inch MN-MO Steel (Heat J-7044)	18
TABLE II	Chemical Composition and Detonation Velocity of Explosives	19
TABLE III	Direct Explosion Tests of 12 x 12, 18 x 18, and 24 x 24 x 1-inch MN-MO Steel	20
TABLE IV	Influence of Plate Support on Shock Capacity of 18 x 18 x 1-inch MN-MO Steel	21
TABLE V	Influence of Detonation Velocity on Shock Limit of 18 x 18 x 1-inch MN-MO Steel	22
TABLE VI	Influence of Detonation Velocity on Shock Limit	23
TABLE A-1	Direct-Explosion Tests of 12 x 12, 18 x 18, and 24 x 24 x 1-inch Low-Alloy NI-CR Steel Plate	A-4

LIST OF FIGURES

	<u>Page</u>
FIG. 1	Experimental Procedure for Conducting Explosion Test 24
FIG. 2	Primacord Initiator Designed to Produce Flat Detonation Wave 25
FIG. 3	Standard Density Apparatus 25
FIG. 4	Typical Microstructures of MN-MO Hull Steel 26
FIG. 5	Influence of Temperature on V-Notch Charpy Impact Strength of MN-MO Hull Steel 27
FIG. 6	Influence of Plate Size on Shock Limit of MN-MO Hull Steel 27
FIG. 7	Deformation of 1-Inch Hull Steel Produced by Shock Limit Charges of Explosive Having Detonation Velocity of 3270 Meters Per Second 28
FIG. 8	Methods for Supporting Test Plates 29
FIG. 9	Influence of Detonation Velocity on Shock Limit 30
FIG. 10	Influence of Detonation Velocity on Dish at Shock Limit Charges 30
FIG. 11	Influence of Detonation Velocity on Deformation at Shock Limit Charges 31
FIG. 12A & 12B	Schematic Representation of Path of Fracture Resulting from Explosive Charges 32
FIG. 13	Typical Failures on Tension Face of 18 x 18 x 1-inch Steel Plate Resulting from Charges in Excess of Shock Limit 33
- - - - -	
FIG. B-1	Arrangement for Determining Detonation Velocity B-3 (See Appendix B)

GLOSSARY

1. Direct-explosion test - a test of steel plate in which the force to produce deformation arises from the detonation of a measured charge of high-explosive powder in contact with the plate under test.
2. Rate of detonation or shock velocity - the rate of propagation of the shock wave produced by the detonation of the explosive charge. This shock wave is transmitted to the plate and the primary stress waves therein are initially assumed to have this velocity.
3. Dish - the hemispherical-like deformation of the test plate produced by the explosive forces. Dish is measured from a straight edge placed across opposite edges of the plate to the center of impact and is expressed in millimeters.
4. Shock limit - the weight of explosive required to produce maximum deformation of test plate without visible cracking.

SUMMARY

A preliminary investigation was conducted to develop optimum test procedures for evaluating the shock resistance of high yield strength structure steel. The significant results are listed below.

1. The minimum size test plate that can be expected to behave like a large plate when subjected to explosive loading is 18" x 18" x t inches in dimension.
2. The shock limit for Mn-Mo steel is the same whether the test plate is supported along all four edges by loose bars arranged in pinwheel configuration or by a rigid welded box-like frame.
3. There is no significant difference in shock limit when the support bars rest on a steel plate on a massive concrete foundation, or on a steel plate lying on firm earth. The concrete foundation, or base, is considered more satisfactory because its rigidity is reproducible and does not change as soil does with changing weather conditions.
4. The shock limit decreases as the detonation velocity of the explosive charge used for testing increases. For example, the shock limit for Mn-Mo heat treated steel is 1000 grams for an explosive having a detonation velocity of 2144 meters per second and 580 grams for a powder with a detonation velocity of 4148 mps.
5. As the detonation velocity of the explosive used for testing increases, the dish, or deformation of the plate which can occur without visible fracture decreases, i.e., with explosives having detonation velocities of 2144 and 4148 mps, the dish is 63 and 51 mm, respectively for heat treated steel tested with shock limit charges.
6. Over the entire range of detonation velocities of the explosives used, failure in the heat treated Mn-Mo steel was similar to a spall.

The crack on the tension face of the test plate usually extended along a circle approximately four inches in diameter and concentric about the vertical centerline of the explosive. With excessive charges similar cracking occurred on the compression side of the plate but the circle about which the crack extended was approximately one inch in diameter. Depending upon the severity of the charge, the cracks extended either partially or completely around the four-inch circle. When the crack extended around the entire periphery, a circular piece of the full thickness of the plate was dislodged. This piece shows characteristic shear fractures at both faces which extend inward approximately one-quarter of an inch with the remainder exhibiting cleavage fracture. Because of the nature of the fracture, its origin was not definitely apparent but observation shows that it is located approximately one quarter inch below the compression face of the plate and somewhere near the periphery of the one-inch circle about which the compression face of the large plate usually cracked.

7. Although in any one series of tests with a single batch of powder the consistency of results is excellent, a few anomalous results have been observed which require further investigation. In testing the Mn-Mo steel, the shock limit was established at 800 grams with one lot of powder having a detonation velocity of 3245 mps and 650 grams with another lot having almost identical detonation velocity, 3250 mps. Whether this discrepancy may be attributed to the explosive or to differences in the steel, particularly the heat treatment, should be investigated.

INTRODUCTION

The failure of ships in service has focussed attention on the "brittle" nature of steels heretofore considered ductile. Recent investigations show that some steels which may be considered ductile on the basis of conventional mechanical tests are extremely brittle under high velocity shock loading, or under loading which involves complex multi-axial stresses, particularly at low temperatures. Furthermore, the degree of brittleness in service varies widely among steels of almost identical chemical composition, hardness, and ductility, the latter property being represented by deformation measured in the tensile or bend test at room temperature.

Considerable interest has been shown in the development of a test which is capable of evaluating the performance of steels subjected to severe forces resulting from shock loading, and developing in rigid welded structures operated at low temperature.

The direct-explosion test developed during World War II shows promise of being capable of discriminating between shock resistant and shock-sensitive steels which cannot be distinguished by regular testing methods. This relatively simple test is conducted by detonating a measured explosive charge having a known detonation velocity, or velocity of shock wave, in contact with a test plate supported horizontally along all four edges. The maximum weight of the explosive charge which a plate so tested can withstand without visible cracking is considered a measure of the ability of the plate material to satisfactorily perform under severe service conditions.

In the past, the performance of prime steel as evaluated by the V-notch Charpy impact test has been correlated with performance under high velocity shock such as is encountered in ballistic tests using blunt solid projectiles. The

velocity of the projectiles in these tests ranged from approximately 750 to 2500 feet per second. Although this is considered "high velocity" when compared to the relatively low velocity of the Charpy test, it is low when compared to shock waves arising from explosions which have a propagation rate within the range from approximately 6000 to 16,000 feet per second. To date, there has been no direct correlation between low temperature Charpy impact results and resistance to deformation at these high shock velocities.

The direct-explosion test shows merit in its ability to evaluate the performance of welded joints for several reasons. Heretofore, estimation of the shock performance of even a simple welded structure required that the specific properties of prime plate, weld metal, and the individual zones at the heat-affected region be established by a series of concurrent tests at different temperatures and that these results then be interpreted in terms of the overall response of the joint. With the direct explosion test the necessity for the above procedure is obviated, since the test simultaneously evaluates the various regions of the plate and weld in such a manner that the result indicates the ability of the weldment to withstand severe loading conditions.

Summarizing, the direct-explosion test possesses certain advantages over other tests, e.g., the V-notch Charpy impact test, because it is relatively simple, may be applied to full thickness plate, and is capable of evaluating the overall performance of welded joints.

Further development of the direct-explosion test procedure has been undertaken to ascertain the optimum size of test plate, the type of support for the test plate which yields most consistent results, and the type of explosive to be used in subsequent phases of this investigation.

The originally proposed program of investigation to evaluate the shock

properties of marine constructional steels is outlined below:

1. Determine the effect of plate size on the quantity of explosive required to fracture a given type of plate.
 - a. Using one-inch low-alloy Ni-Cr plate to determine the amount of charge required to just crack the following:
 - 1) 12 x 12-inch test plate
 - 2) 18 x 18-inch test plate
 - 3) 24 x 24-inch test plate
 - 4) 30 x 30-inch test plate

(The test plate is supported on four sides and rests on a heavy rigid base plate. Tests to be conducted using powder having a detonation velocity of 3200 meters per second; 105-mm diameter charge).
2. Determine the effect of rigidity of support on the amount of powder required to just produce cracking in optimum size test plates as determined in above (same steel and explosive as used in 1).
 - a. Loose frame; heavy concrete block and armor support
 - b. Rigid frame; heavy concrete block and armor support
 - c. Loose frame; 36 x 36 x 1-inch armor support on firm earth
 - d. Rigid frame; 36 x 36 x 1-inch armor support on firm earth
3. Evaluate the shock resistance of one-inch Mn-Mo quenched and drawn plate, using test plate size and support determined above, as follows:
 - a. Determine the quantity of powder required to just fracture this steel at 70°F using a powder with a detonation velocity of 3200 meters per second.
 - b. Repeat 3a with 4,000 meter per second powder and with higher detonation velocity until spalling is produced in the plate material.

- c. With standardized powder, (detonation velocity just below that required for spalling) determine the weight of charge which just produces fracture at four temperatures to determine whether or not transition effects exist in this test.
4. Repeat phase 3 above for other steels in the program.
5. Determine the effect of welding on shock performance of one-inch Mn-Mo austenitized, quenched, and tempered plate and of other selected steel.
 - a. Variables to be investigated
 - 1) Electrode composition and coating
 - 2) Joint design and pass sequence
 - b. The specimens to be used in this investigation are to be of the single "I" weld type
 - c. All tests are to be conducted at 70°F
 - d. The preheat given these specimens will be dictated by the results of the work on electrodes now being conducted at the Philadelphia Naval Shipyard
 - e. Work on specimens fabricated with submerged melt and those subjected to various stress relieving processes is to be deferred
6. The origin of fracture of plates tested is to be determined. Selected samples of the various types of fractures encountered in this work will be examined.
7. A theoretical study of the stresses produced by the explosion of a charge of powder on a plate is to be made. To assist in this analysis, the experimental data listed below may be helpful. The assistance of the David Taylor Model Basin staff will be requested in carrying out this experimental program.

a. High speed motion picture studies of the reactions of the plates to an explosion

b. Strain gage studies of the reaction of a plate to an explosion

This program was approved by the SR-25 Advisory Committee, Committee on Ship Construction, National Research Council, on March 3, 1948.

A similar investigation is being sponsored by the Department of the Army to evaluate shock resistance of thinner materials.

DETAILS OF THE DIRECT-EXPLOSION TEST

In conducting the direct-explosion test, a square plate specimen is continuously supported along its four edges by means of four cold-rolled-steel bars arranged in pinwheel fashion as shown in Fig. 1-A. These bars in turn rest upon two large steel plates, the lower three inches thick and the upper one inch thick, which weigh approximately 2500 pounds and rest on a massive steel reinforced concrete base. The square opening provided by the 2.5 x 4-inch rectangular supporting bars is 16 x 16 inches for 18 x 18-inch specimens, thereby providing one-inch overlap along the four sides of the specimen. The symmetrically supported specimen is shown in Figure 1-B. Previous work indicated that a firm base on which the specimen and related supports could be placed is necessary to eliminate inconsistencies in the test.

A cylindrical paper container, 105 millimeters in diameter, containing a given quantity of explosive packed to a definite density is then centered in direct contact with the surface of the plate as shown in Fig. 1-C. A cut-away section revealing the explosive in the container is shown in Fig. 1-D.

A special initiator is then placed in contact with the center of the top section of the explosive, also shown in Fig. 1-D. This initiator consists of a 1.5-inch diameter ring of Ensign-Bickford Primacord with a piece extending

across the center of the ring, both firmly attached to a wooden plug as shown in Fig. 2. One end of each of two lengths is bent in the form of a semi-circle to make a ring with the opposite end of one of these pieces twisted around the extending portion of the other. A suitable detonator is attached to the extending piece of Primacord.

When the detonator is fired, the length of Primacord detonates, which in turn activates the explosive charge. The use of the flat ring initiator produces an essentially flat detonation wave originating from a plane rather than a point.

The powder and initiator assembly is placed in a large cylindrical paper container, Fig. 1-E, which is then filled with screened Ottawa sand, Fig. 1-F. This paper container is 8.5 inches in diameter and 12 inches high and, when filled, holds approximately 35 pounds of 20-30 mesh sand. The sand acts as a confinement, increases reproducibility of the test, and permits the use of a smaller charge to produce a given force than when no confinement is used. Fig. 1-F shows the completed assembly ready for detonation.

In considering the explosive used for testing, it is necessary to examine the general effects of explosives in producing damage. These effects may be conveniently classed as brisant effects and gas-volume effects, the inter-relationship of which is complex and which provides the many variations in shock produced by explosive action. A highly brisant explosive produces a shattering blow which, when applied to steel plate, usually tends to produce failure parallel to the surface of the plate, or "spalling" directly beneath the location of maximum impact energy. Explosives with high brisance have a rapid detonation rate. On the other hand, an explosive with low brisance, or low rate of detonation, tends to produce deformation in the vicinity of the application of the

explosive force and tends to fracture steel plate in a direction normal to the plate surface. Actual behavior of a given steel subjected to the action of a specific explosive necessarily depends upon both the characteristics of the powder and the properties of the plate.

The gas volume of an explosive may be likened to the mass of a projectile in flight. Explosives possessing high gas volume for a given rate of detonation will impart more energy when detonated than corresponding explosives with low gas volume. Similarly, the detonation velocity of an explosive may be likened to the speed of a projectile. A variety of projectile weights and velocities may be used in ballistics to fracture a given armor; likewise, the gas volume and rate of detonation of explosives may be varied, within reasonable limits, to accomplish the same purpose. The ballistics analogy provides a convenient though over-simplified physical picture of the rate of detonation and gas volume effects in explosives.

In general, the direct-explosion test is conducted so that an explosive with a detonation velocity or brisance which just avoids producing a spalling type failure is used in testing a particular material. Gas volume effects appear less important but, in general, a powder with a high gas volume is considered desirable. By keeping the rate of detonation of the explosive at a maximum without producing spalling, it is believed that the most severe test condition is provided.

When the direct-explosion test is used as a discriminator to ascertain differences in shock sensitivity, a group of five to ten plates is tested under controlled conditions to determine the maximum weight of a given explosive of fixed density which will deform the plate without visible fracture on the tension face. The "shock limit" is then established by repetitive tests for that amount of powder which will just avoid producing a visible crack on the tension side of

the plate under test. Thus, the shock resistant properties of various steels are established in terms of the "shock limit" which is expressed in terms of weight, in grams, of the explosive used.

The special explosives used in testing various types of steel plate usually contain trinitrotoluene as a basic ingredient with ammonium nitrate and sodium nitrate as cooperating oxidants, aluminum powder, and oil. In order to insure satisfactory characteristics, it is essential that the ingredients be carefully selected and the particle size and the degree of mixing be carefully controlled. The properties of the various explosives are evaluated by tests of rate of detonation, standard density, gas volume, and lead block compression.

After an explosive has been formulated and selected for a particular series of tests, a predetermined amount is packed in the 105-millimeter-diameter cylindrical paper container in small increments, each of which is tamped to a controlled density using the apparatus shown in Fig. 3.

MATERIAL

STEEL

The two plates of one-inch low-alloy nickel-chromium steel submitted for tests outlined in Phases 1 and 2 of the program were apparently from two different heats and were sufficiently different in shock resistance that the trends shown by the direct-explosion test were not conclusive. This material was discarded and Phases 1 and 2 were repeated using another steel. The tests conducted on the low-alloy Ni-Cr material are described in Appendix A of this report.

Phases 1 and 2 of the program were repeated and the remainder of the program is being investigated with one-inch manganese-molybdenum steel of the

following chemical composition.

Carbon	0.17%
Manganese	1.21
Silicon	0.31
Sulfur	0.028
Phosphorus	0.021
Nickel	0.11
Chromium	0.02
Molybdenum	0.19
Copper	0.12
Aluminum	0.021
Boron	0.001/0.002

Heat Treatment - This Mn-Mo steel was supplied in 180 x 60 x 1-inch pieces heat treated in the following way.

Heated in a continuous furnace for a total time of two hours, held forty-five minutes at a temperature of 1625 to 1650°F; quenched using water cooled platens; drawn at 1215°F for four hours.

Microstructure - Microscopic examination of two samples from this heat of material reveals:

- a. The microstructure of one sample comprises a uniform dispersion of fine carbide in a ferrite matrix, Fig. 4-A. This structure apparently results from the tempering at 1215°F of an almost completely martensitic structure obtained by platen-quenching. A few areas of acicular ferrite are noticeable, indicating that a small amount of the austenite had transformed at approximately 1000°F on cooling. The hardness of this specimen is 204 BHN (range 194-214).
- b. The microstructure of the other sample comprises a less uniform dispersion of fine carbide in a ferrite matrix, Fig. 4-B. Considerably more acicular ferrite is noticeable in this specimen. Apparently, the structure of this specimen, after platen quenching

and before tempering, was martensite and a Widmanstätten-type aggregate of ferrite and carbide. Tempering this structure tends to agglomerate the carbide resulting in a less uniform structure than in the one described above. The hardness of this specimen is 203 BHN (range 197-205).

Although these specimens have almost identical hardness, the differences in the structure could conceivably cause wide differences in shock behavior.

Mechanical Properties -

Tensile Test: Results of tensile tests of 0.505-inch diameter specimens of the Mn-Mo steel are listed below.

	<u>Longitudinal*</u>	<u>Transverse*</u>
Ultimate tensile strength, 10^3 psi	97.2	95.7
Yield strength, 10^3 psi		
Drop of beam	84.8	83.8
0.2% offset	82.6	83.2
Elongation in 2 inches, %	21.2	21.3
Reduction in Area, %	67.5	67.4

*With respect to rolling direction

V-Notch Charpy Impact Test: Specimen bars were cut from the plate transverse and longitudinal with respect to the rolling direction. The bars were notched such that the axis of the notch was parallel to the thickness dimension of the plate. The base of each notch was ground with 600 mesh carborundum to eliminate milling cutter scratches.

Results of impact tests at 72, 32, -4, -40, -76, -107; and -319°F (22, 0, -20, -40, -60, -77, and -195°C) are listed in Table I and shown graphically in Fig. 5. At each test temperature, the impact strength of the longitudinal and the transverse test bars is

essentially the same indicating that the plate does not have directional properties. This is further indicated by the type of fracture observed in the direct explosion test discussed in a later section. At several temperatures the range of impact values is wider than is usually expected. These data were checked with another series of specimens and again the range was as wide. The inflection point of the temperature-impact strength curve appears to be located at -40°F at an impact strength of 45 to 50 ft-lb.

EXPLOSIVES

The explosives compounded for this program consist of trinitrotoluene (TNT) with sodium nitrate and ammonium nitrate. The composition and detonation velocity of each explosive used is listed in Table II.

The method for determining the detonation velocity of an explosive charge is described in detail in Appendix B of this report.

RESULTS OF DIRECT-EXPLOSION TESTS

The results of direct-explosion tests are reported phase by phase of the program outlined in the introduction with the exception that Mn-Mo steel was used throughout.

1. Determine the effect of plate size on the quantity of explosive required to fracture a given type of plate.

The shock limit of 12 x 12-, 18 x 18-, and 24 x 24 x 1-inch test plates of this Mn-Mo steel is, respectively, 670, 780, and 780 grams of explosive having a detonation velocity of 3270 meters per second, Table III and Fig. 6. The shock limit for 18 x 18 and 24 x 24-inch test plates is the same indicating that there is no advantage in testing specimens larger than 18-inch square.

Photographs of a plate of each size tested with shock limit charges are shown in Fig. 7.

2. Determine the effect of rigidity of support on the amount of powder required to just produce cracking in optimum size test plates as determined from Phase 1, above.

Four series of 18 x 18 x 1-inch plates were screened with an explosive possessing a detonation velocity of 3250 meters per second. Two sets of these plates, F12 and F13, Table IV, were tested with the supporting bars resting on steel plates on the concrete foundation. The other two sets, F14 and F15, Table IV, were tested with supporting bars resting on a steel plate on firm earth. Series F12 and F14 were screened with the supporting bars placed in pinwheel configuration, Fig. 8A. Series F13 and F15 were screened with the supporting bars fabricated in a boxlike frame by welding, Fig. 8B.

Results of these tests, Table IV, indicate that there is no difference in shock limit when loose support bars or a welded frame is used. Furthermore, reliable tests can be conducted with support bars resting on a one-inch steel plate lying on firm earth, but should several days pass between series of tests, discrepancies in results may be observed if the "dryness" of the earth changes with the weather. The shock limit of these four series of tests is essentially the same as that established in Phase 1 with an explosive having a rate of detonation of 3270 meters per second.

3. Evaluate the shock resistance of the subject material using test plate size and support determined above. (Influence of detonation velocity on shock limit.)

Screening tests of 18 x 18 x 1-inch Mn-Mo plate supported by

loose bars in pinwheel configuration on steel plates over the concrete base with explosives having detonation velocities of 2144, 3250, 3740, and 4148 meters per second indicate that as detonation velocity increases, the shock limit and deformation at shock limit charges decreases. Results of these screening tests are listed in Table V and summarized in Table VI and Fig. 9 and Fig. 10. Photographs of plates tested with shock limit charges of velocity are shown in Fig. 11.

The data plotted in Figs. 9 and 10 lie within a band bounded by two parallel lines indicating that a range of values for shock limit and dish at any detonation velocity is approximately 150 grams and 8 millimeters, respectively. This range appears to be excessive for the reproducibility of tests for each batch of powder is well within twenty grams for shock limit and 3 or 4 millimeters for dish.

It is believed that these anomalous results may be attributed to the heat treatment of the steel or, possibly, to some specific property of the explosive such as gas volume and must be thoroughly investigated before further testing is continued.

Mode of Failure of Mn-Mn Steel in the Direct-Explosion Test

The mode and the locus of fracture of this material at or slightly above shock limit charges is essentially the same over the entire range of detonation velocities, 2144 to 4148 mps. Failure apparently starts about a quarter of the way through the plate near the compression face and on the periphery of approximately a one-inch circle and propagates radially almost parallel to the plate faces to the periphery of a four-inch circle where the fracture penetrates to the tension face. This description of the mode of failure is based on examination of pieces dislodged by higher charges. In all cases, the

path of fracture parallel to the plate faces is by cleavage and connecting both tension and compression faces with this parallel brittle fracture, where such complete failure occurs, is a shear failure exhibiting high ductility as shown schematically in Fig. 12A. Thus, failure apparently occurs from within the plate to the tension and compression faces. This is subject to confirmation when partially broken plates are sectioned for further study.

With higher charges at each detonation velocity, several cracks radiate from the center of impact. The surface of the cracks is almost perpendicular to the plate surface and shows shear failure at the plate faces and cleavage or brittle failure between them as shown schematically in Fig. 12B.

Typical fractures on the tension face and resulting from charges in excess of the shock limit are shown in Fig. 13.

BIBLIOGRAPHY

1. W. O. Snelling, "Direct Explosion Test for Welded Plate", Progress Report, OSRD No. 1206, Serial No. M-41, NDRC Research Project NRC-25, Feb. 10, 1943.
2. W. O. Snelling, "Direct Explosion Test for Welded Armor Plate, Part I - Development of Direct Explosion Test Equipment and Procedure", Progress Report, OSRD No. 2083, Serial No. M-163, NDRC Research Project NRC-25, Nov. 23, 1943.
3. W. A. Snelling and W. O. Snelling, "Direct Explosion Test for Welded Armor and Ship Plate, Part I - Armor Plate", Final Report, OSRD No. 4655, Serial No. M-446, NDRC Research Project NRC-25, Jan. 23, 1945.
4. W. A. Snelling and W. O. Snelling, "Direct Explosion Test for Welded Armor and Ship Plate, Part II - Prime and Welded Plate", Final Report, OSRD No. 6382, Serial No. M-622, NDRC Research Project NRC-25, Dec. 5, 1945.
5. W. A. Snelling, "Direct Explosion Test for Welded Armor and Ship Plate: Prime and Welded Plate", Bureau of Ships, Navy Department, Contract NObs-31223, Final Report, Serial No. SSC-4, Aug. 30, 1946.
6. A. Muller, W. G. Benz, W. A. Snelling, "Preliminary Investigation of the Shock Resistance and Mechanical Properties of 0.5-inch Cr-Mo-V Aircraft Armor", Progress Report No. 1, WAL 110/13-9, May 1948.

TABLE I - V-NOTCH CHARPY IMPACT STRENGTH OF ONE-INCH MN-MO STEEL
(HEAT J-7044)

Test Temperature		Impact Strength, Ft.-Lb.	
<u>°F</u>	<u>°C</u>	<u>Range</u>	<u>Average</u>
<u>Longitudinal Test Bars</u>			
72	22	66-77	71.5
32	0	48-91	64.5
-4	-20	72-88	80.7
-40	-40	26-58	43.2
-76	-60	24-40	30.0
-107	-77	11-26	16.2
-319	-195	6-8	6.7
<u>Transverse Test Bars</u>			
	22	74-76	74.8
	0	57-80	71.3
	-20	76-81	79.3
	-40	32-58	48.3
	-60	10-27	18.2
	-77	18-24	21.3
	-195	6-8	7.3

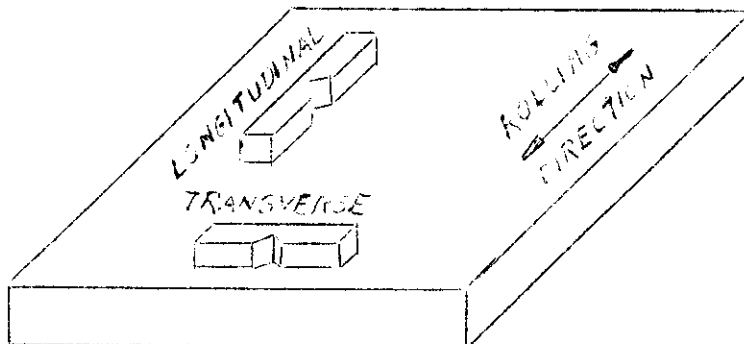


TABLE II. CHEMICAL COMPOSITION AND DETONATION VELOCITY OF EXPLOSIVES

<u>Explosive Designation</u>	<u>CHEMICAL COMPOSITION, %</u>					<u>Detonation Velocity Meters per second</u>
	<u>TNT</u>	<u>NH₄NO₃</u>	<u>NaNO₃</u>	<u>Al</u>	<u>Oil</u>	
TPCo 592	22.0	50.0	23.5	4.0	0.5	2144
T63	18.5	51.0	26.0	4.0	0.5	3245
T52	19.45	50.0	26.05	4.0	0.5	3250
T50	22.0	50.0	23.5	4.0	0.5	3270
T61	26.0	48.2	21.0	4.0	0.3	3740
T15	50.0	23.0	23.0	3.5	0.5	4148

(Note: Explosives designated TPCo 592 and T50 have the same chemical composition but different detonation velocities, 2144 and 3270 mps, respectively. The difference in velocities results from the different techniques used in graining the NH₄NO₃.)

TABLE III - DIRECT-EXPLOSION TESTS OF 12 x 12, 18 x 18, AND
24 x 24 x 1-INCH Mn-Mn STEEL

(Detonation Velocity of Explosive Charge: 3270 mps)

Plate No.	Plate Size in.	Weight of Charge gm	Dish mm	Fracture	Shock Limit gm	Dish at Shock Limit mm
FLAA	12 x 12 x 1	670	59	Yes	670	61
B	"	650	59	No		
C	"	670	61	No		
D	"	680	92	Yes		
E	"	660	58	No		
F	"	620	56	No		
G	"	670	61	Yes		
H	"	670	58	No		
I	"	720	93	Yes		
J	"	660	62	Yes		
FLAB	18 x 18 x 1	790	61	Yes	780	60
C	"	760	59	No		
E	"	1000	—	Yes		
EBX	"	780	60	No		
H	"	780	59	No		
I	"	780	64	Yes		
K	"	760	58	No		
L	"	800	61	Yes		
FLAC	24 x 24 x 1	780	49	No	780	49
B	"	780	49	Yes		
F	"	790	51	Yes		
G	"	790	56	Yes		
H	"	800	52	Yes		

TABLE IV - INFLUENCE OF PLATE SUPPORT ON SHOCK CAPACITY OF
18 x 18 x 1-INCH Mn-Mo STEEL

(Detonation Velocity of Explosive Charge: 3250 mps)

Plate No.	Weight of Charge, gm	Dish mm	Fracture	Shock Limit gm	Dish at Shock Limit mm
-----------	----------------------	---------	----------	----------------	------------------------

Loose Bars Resting on Steel Plate on Concrete Foundation

F12A	790	58	No	800	61
B	820	69	Yes		
C	800	57	No		
D	810	85	Yes		
E	800	58	No		
F	810	80	Yes		
G	800	61	No		
H	800	60	Yes		
I	800	57	No		

Supporting Frame of Welded Bars on Steel Plate on Concrete Foundation

F13A	800	60	No	800	60
B	810	61	Yes		

Loose Bars Resting on Steel Plate on Firm Earth

F14A	810	58	No	780	60
B	820	62	Yes		
C	810	63	Yes		
D	800	62	Yes		
E	790	59	Yes		
F	770	61	No		
G	780	59	No		
H	790	73	Yes		
I	780	—	Yes		
J	750	58	No		
L	750	58	No		
M	760	58	No		
N	770	58	No		
O	790	63	Yes		
P	780	60	No		
Q	790	60	Yes		
R	780	65	Yes		

Supporting Frame of Welded Bars on Steel Plate on Firm Earth

F15A	780	58	No	800	58
B	790	59	No		
C	790	58	No		
D	800	58	No		
E	820	63	Yes		

TABLE V - INFLUENCE OF DETONATION VELOCITY ON SHOCK LIMIT OF
18 x 18 x 1-INCH Mn-Mn STEEL

Plate No.	Detonation Velocity mps	Weight of Charge gm	Dish mm	Fracture	Shock Limit gm	Dish at Shock Limit gm
F17A	2144	1000	62	No	1000	63
B	"	1020	86	Yes		
C	"	1000	63	No		
D	"	1010	68	Yes		
E	"	1010	81	Yes		
F12A	3250	790	58	No	800	61
C	"	800	57	No		
D	"	810	85	Yes		
E	"	800	58	No		
F	"	810	80	Yes		
G	"	800	61	No		
H	"	800	60	Yes		
I	"	800	57	No		
F18A	3740	690	--	Yes		
B	"	650	--	Yes		
C	"	610	79	Yes		
D	"	580	53	Yes		
E	"	570	53	Yes		
F	"	560	53	Yes		
G	"	550	53	Yes		
H	"	530	52	No		
I	"	540	52	No		
J	"	540	52	No		
K	"	550	58	Yes		
F16A	4148	720	--	Yes	580	51
B	"	660	69	Yes		
C	"	600	59	Yes		
D	"	560	51	No		
E	"	580	51	No		
F	"	580	51	No		

TABLE VI. INFLUENCE OF DETONATION VELOCITY ON SHOCK LIMIT

<u>Detonation Velocity</u> mps	<u>Dish</u> mm	<u>Shock Limit</u> gm
2144	63	1000
3250	61	800
3740	52	540
4148	51	580

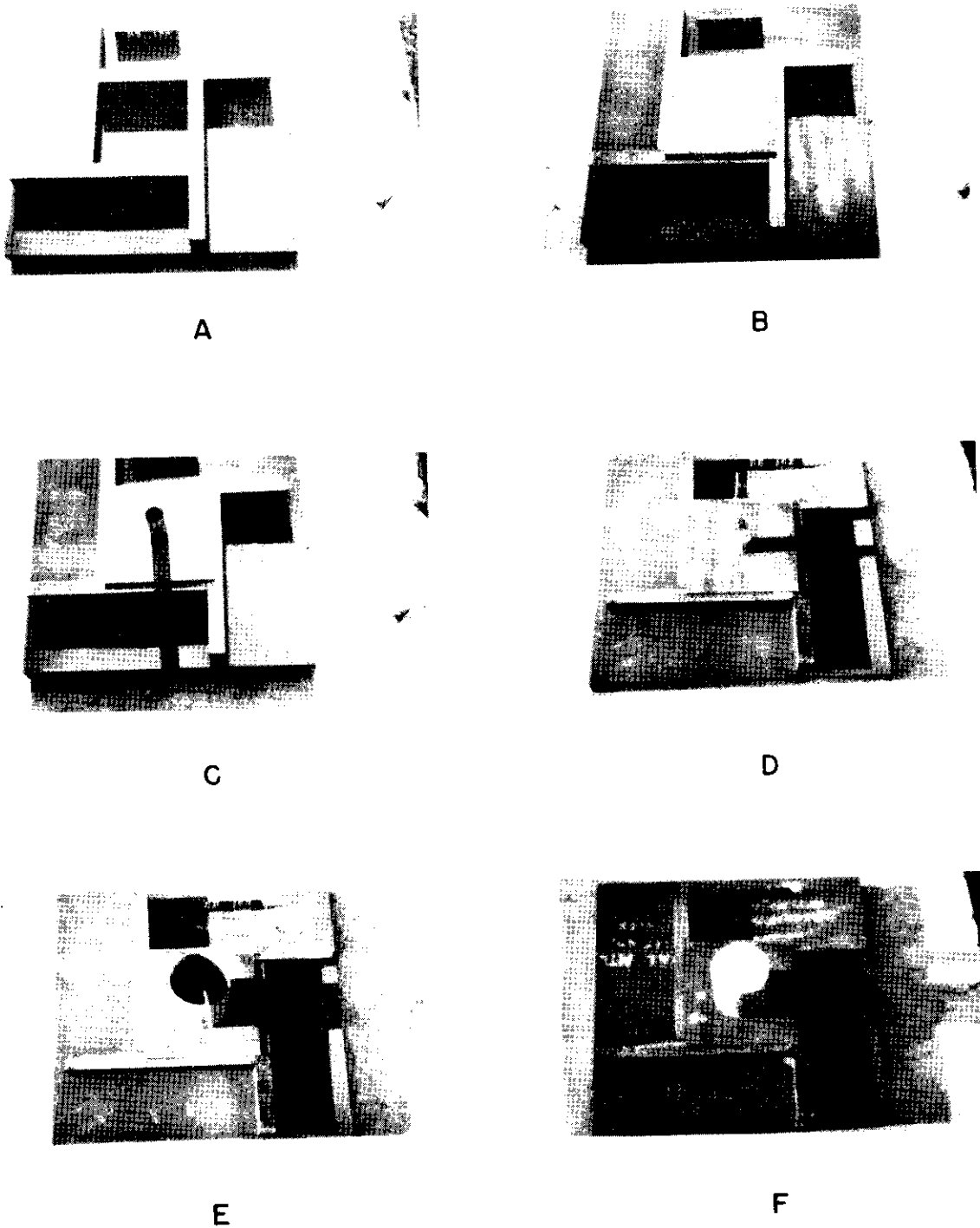


FIG. 1 EXPERIMENTAL PROCEDURE FOR CONDUCTING EXPLOSION TEST

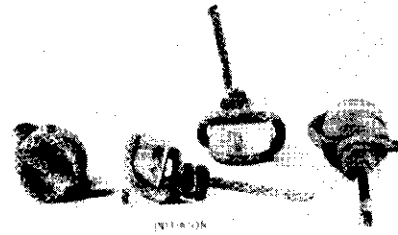


FIG. 2 PRIMACORD INITIATOR DESIGNED TO PRODUCE FLAT DETONATION WAVE.

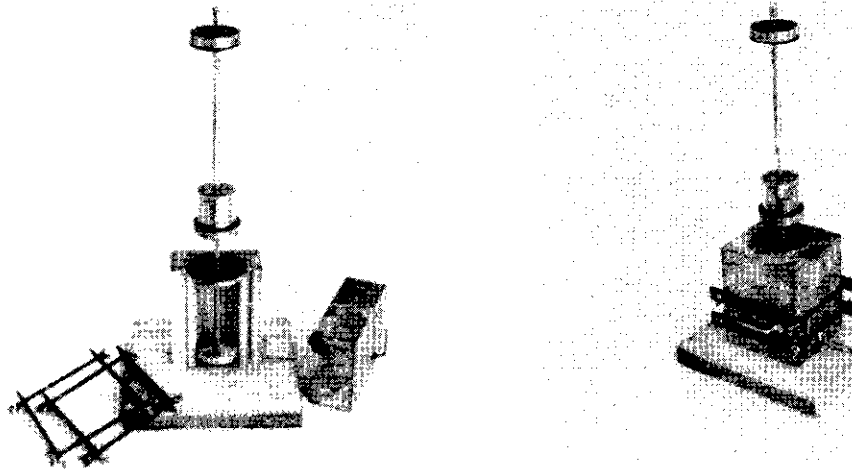


FIG. 3 STANDARD DENSITY APPARATUS.



A



B

FIG. 4 TYPICAL MICROSTRUCTURES OF MN-MO
HULL STEEL (x 500)

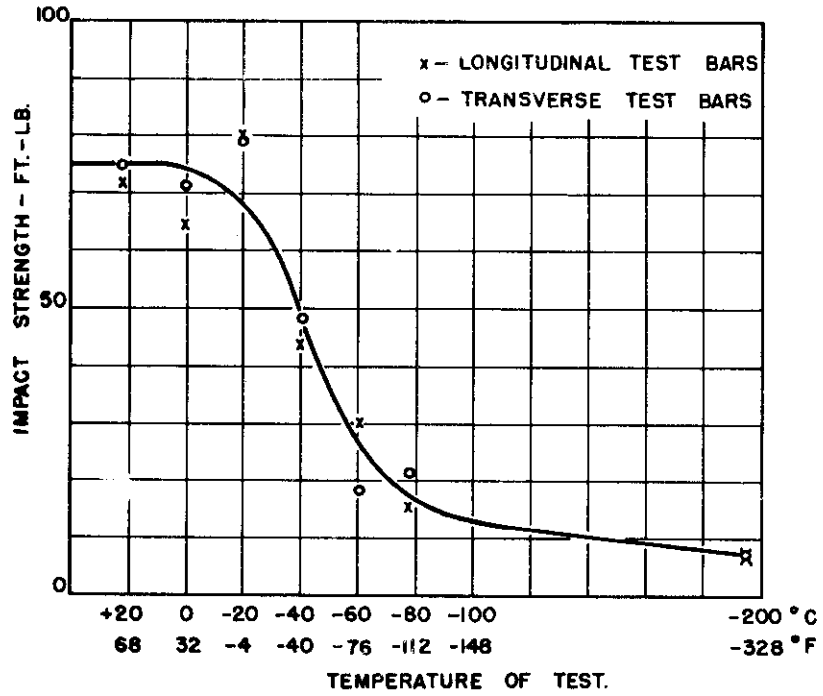


FIG. 5 INFLUENCE OF TEMPERATURE ON V-NOTCH CHARPY IMPACT STRENGTH OF MN-MO HULL STEEL.

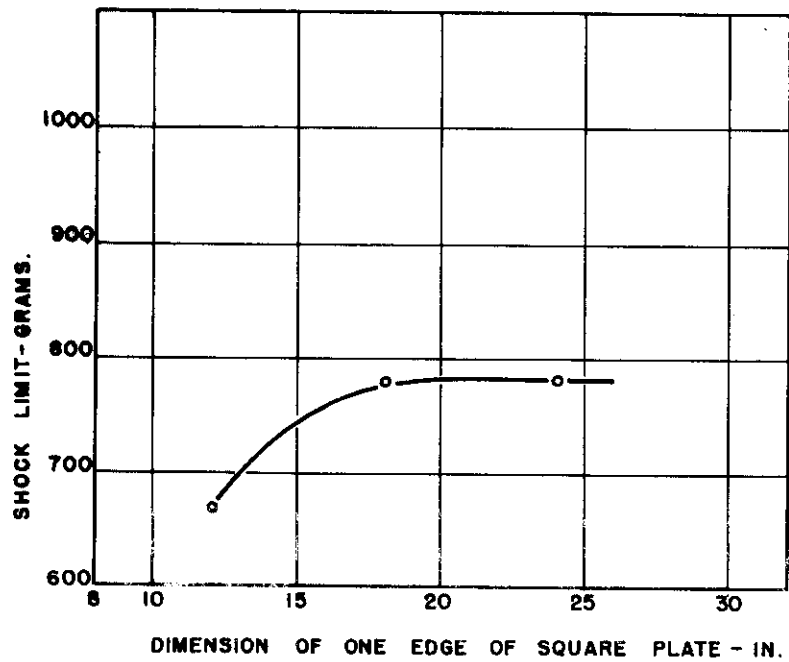
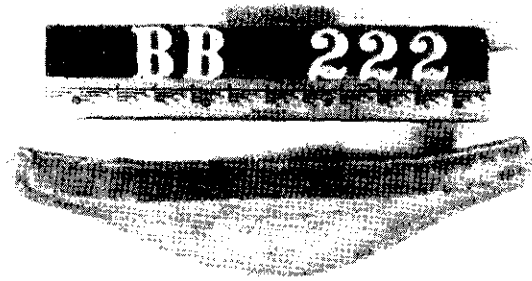


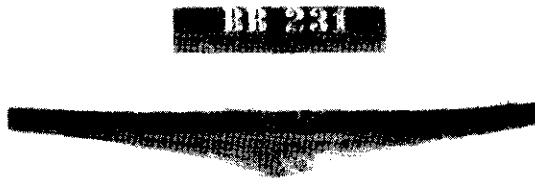
FIG. 6 INFLUENCE OF PLATE SIZE ON SHOCK LIMIT OF MN-MO HULL STEEL (DETONATION VELOCITY 3270 MPS)



12 x 12 x 1 - INCH

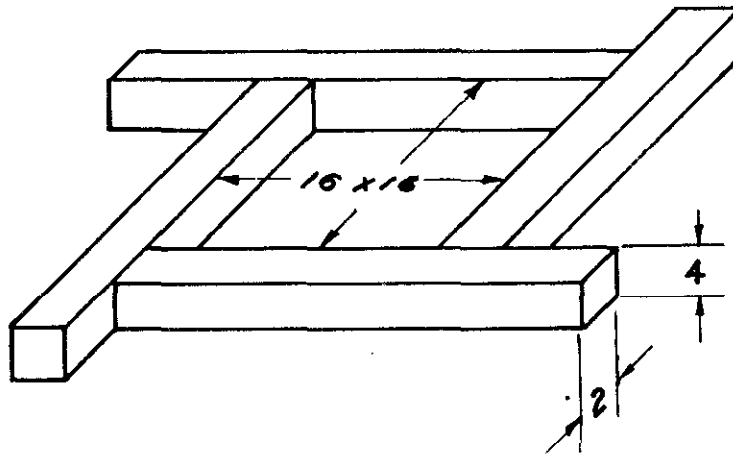


18 x 18 x 1 - INCH

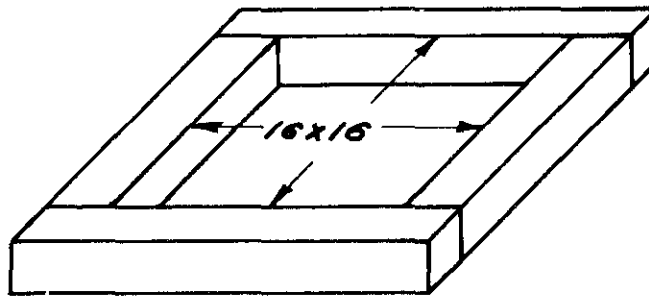


24 x 24 x 1 - INCH

FIG. 7 DEFORMATION OF 1-INCH HULL STEEL PRODUCED BY SHOCK LIMIT CHARGES OF EXPLOSIVE HAVING DETONATION VELOCITY OF 3270 M P S



A - LOOSE SUPPORT BARS



B - WELDED SUPPORT BARS

FIG. 8 METHODS FOR SUPPORTING TEST PLATES

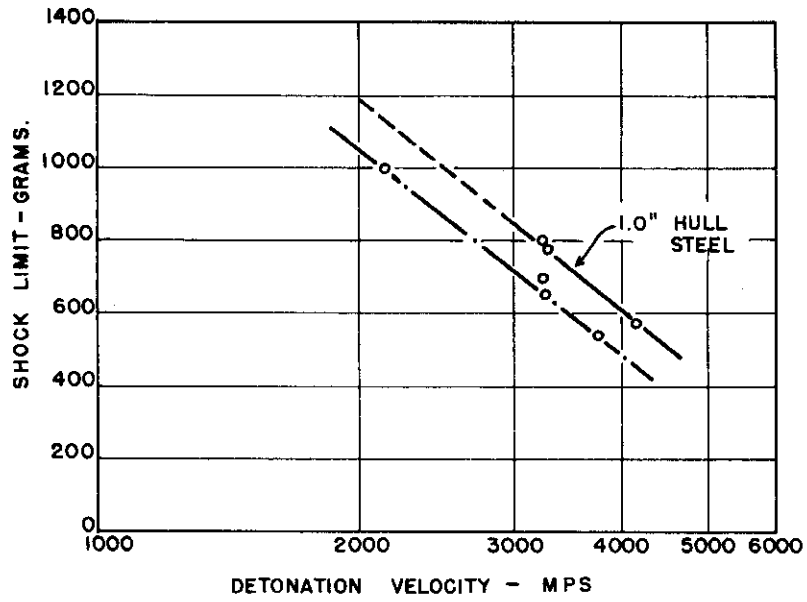


FIG. 9 INFLUENCE OF DETONATION VELOCITY ON SHOCK LIMIT.

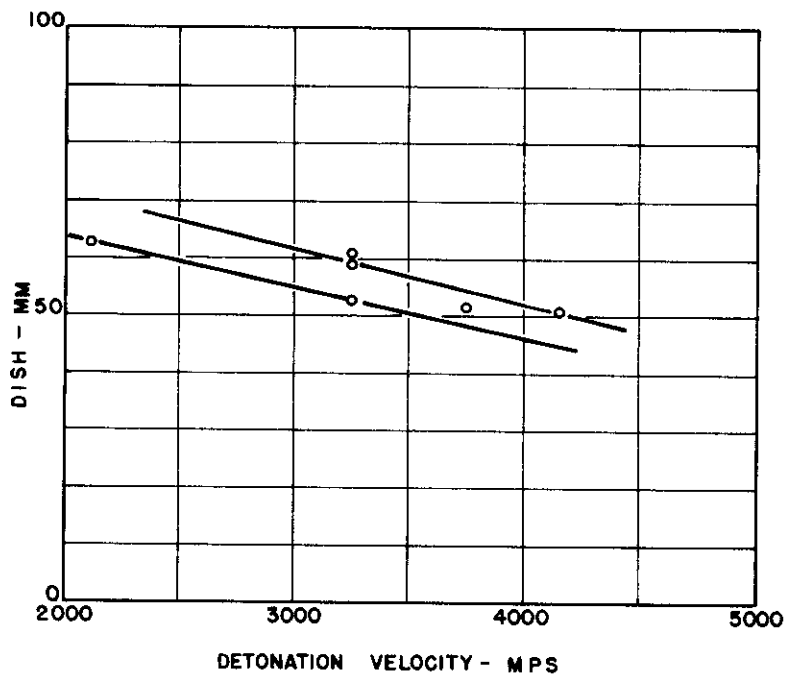
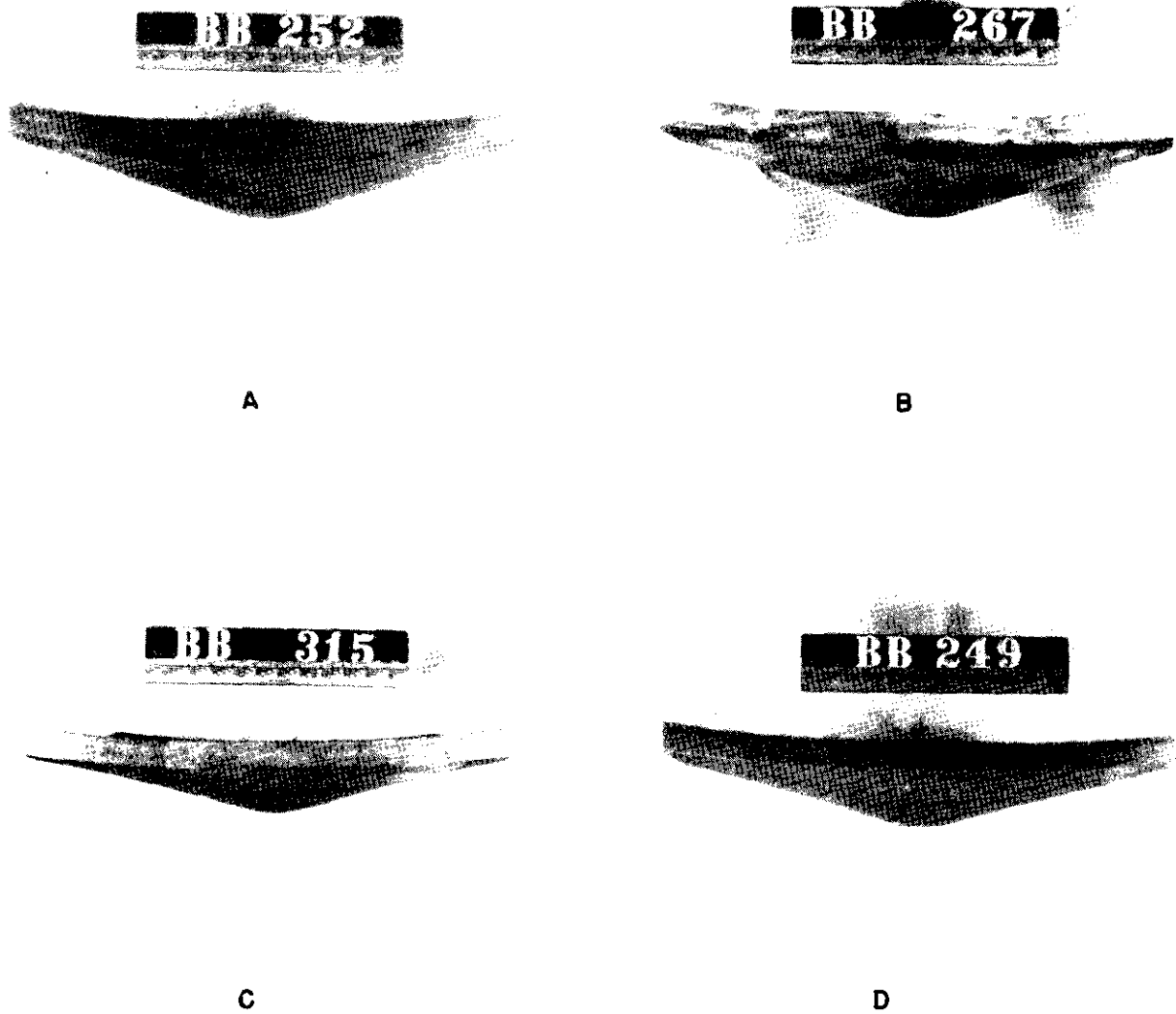


FIG. 10 INFLUENCE OF DETONATION VELOCITY ON DISH AT SHOCK LIMIT CHARGES.



	DETONATION VELOCITY - M PS	DISH - MM
A	2144	62
B	3250	60
C	3740	52
D	4148	51

FIG. 11 INFLUENCE OF DETONATION VELOCITY ON DEFORMATION
AT SHOCK LIMIT CHARGES

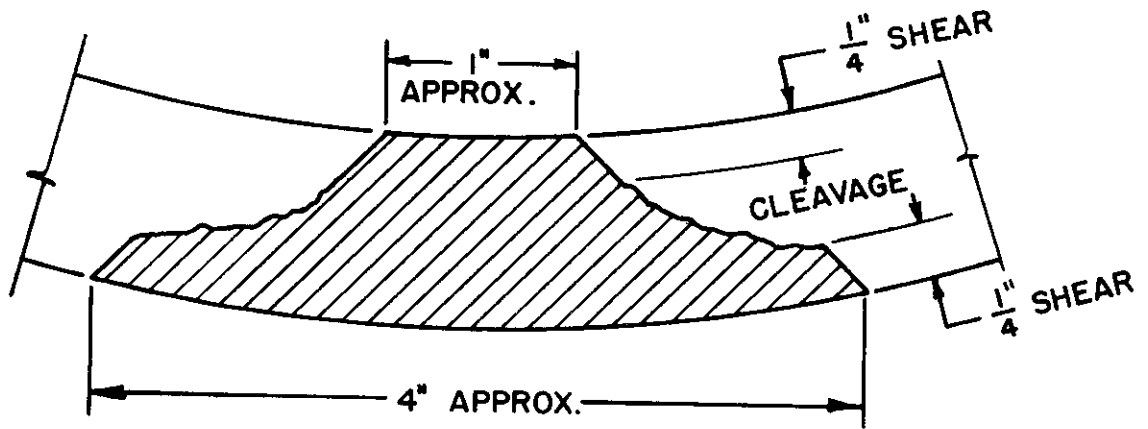


FIG. 12 A SCHEMATIC REPRESENTATION OF PATH OF FAILURE RESULTING FROM EXPLOSIVE CHARGES SLIGHTLY IN EXCESS OF SHOCK-LIMIT WEIGHTS

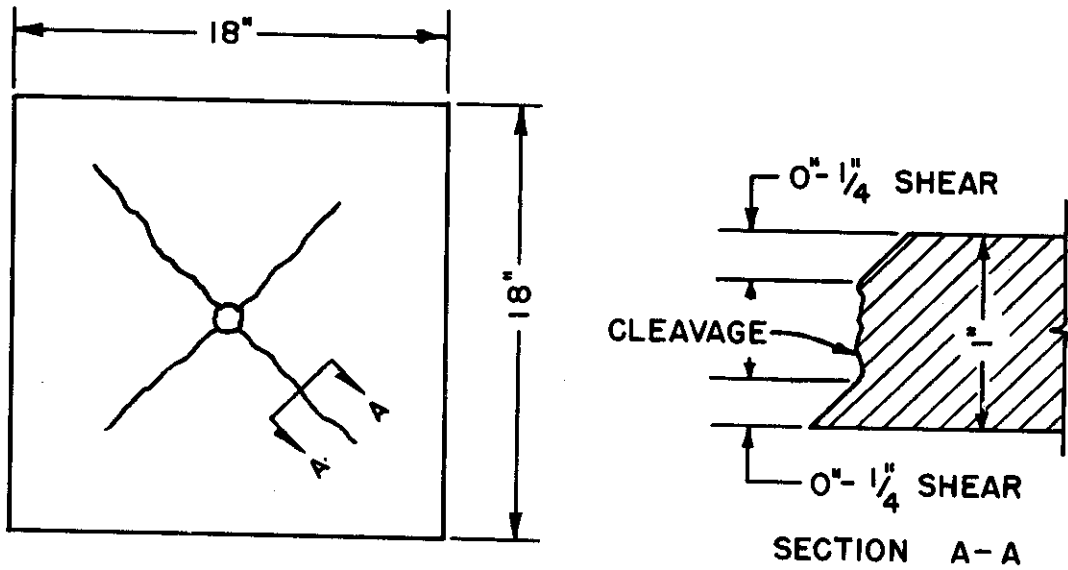


FIG. 12 B SCHEMATIC REPRESENTATION OF CROSS-SECTION OF RADIATING CRACKS RESULTING FROM EXCESSIVE CHARGES

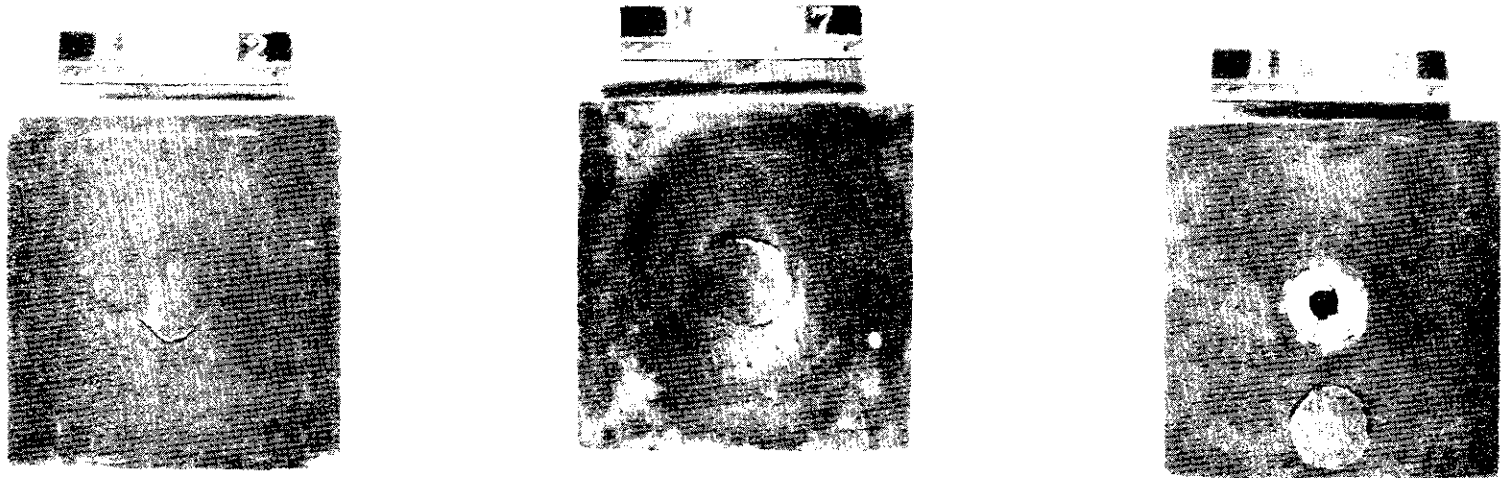


FIG. 13 TYPICAL FAILURES ON TENSION FACE OF 18 x 18 - INCH STEEL PLATE RESULTING FROM CHARGES IN EXCESS OF SHOCK LIMIT.

APPENDIX APRELIMINARY INVESTIGATION OF INFLUENCE OF SIZE OF TEST PLATE
ON SHOCK LIMIT OF ONE-INCH LOW-ALLOY Ni-Cr STEELINTRODUCTION

Originally, Phase 1 of the test program outlined in this report specified that the influence of plate size on the quantity of explosive required to fracture a given type of plate be conducted with low-alloy Ni-Cr steel.

Direct-explosion tests indicated that the two plates of Ni-Cr steel submitted for test were not the same. A comparison of the shock limit of 12 x 12, 18 x 18, and 24 x 24 x 1-inch test plates of this material, therefore, could not be made. Impact tests at 70 and -40°F tend to confirm the difference in behavior of specimens cut from these two plates.

The chemical composition of the two is listed below.

	<u>Plate No. 60</u>	<u>Plate No. 61</u>
Carbon	0.26%	0.23%
Manganese	0.18	0.20
Silicon	0.02	0.02
Phosphorus	0.014	0.017
Sulfur	0.030	0.024
Nickel	2.99	2.76
Chromium	1.22	1.2
Molybdenum	0.04	0.04
Copper	0.04	0.06
Aluminum	< 0.01	0.01

Manufacturing and heat treating data for these two pieces of alloy steel were not available.

MECHANICAL TEST RESULTS

Tensile properties of 0.505-inch diameter specimens of this low-alloy Ni-Cr steel are listed below.

	<u>Plate No. 60</u>	<u>Plate No. 61</u>
Ultimate tensile strength, 10^3 psi	116.2	118.2
Yield strength, 0.2% offset, 10^3 psi	102.0	105.5
Elongation in 2 inches, %	24.8	24.1
Reduction in area, %	64.5	63.0

Results of V-notch Charpy impact tests are listed below.

<u>Plate No.*</u>	<u>Impact Strength, ft-lb.</u>		
	<u>70°F</u>	<u>-40°F</u>	<u>-320°F</u>
60-A	128	120	14.1
61-A	105.5	96.5	10.8
60-B	90.2	92.2	9.9
61-B	92.2	85.5	10.3

* "A" specimens have notch parallel to plate surface and perpendicular to direction of rolling. B specimens have notch perpendicular to both plate surface and direction of rolling.

EXPLOSIVE

The explosive used in this series of tests was similar to those described earlier in this report. The chemical composition is listed below.

<u>Explosive</u>	<u>Chemical Composition, %</u>					<u>Detonation Velocity, mps</u>
	<u>TNT</u>	<u>NH₄NO₃</u>	<u>NaNO₃</u>	<u>Al</u>	<u>Oil</u>	
T46	24.0	49.0	22.7	4.0	0.3	3512

The density of the charges used to test plates varied within the range of 1.224 to 1.257 grams per cubic centimeter.

DIRECT-EXPLOSION TESTS

The results of direct-explosion tests of this material are listed in Table A-1. Results of tests with an explosive having a detonation velocity of 3512 meters per second indicate:

1. The shock limit of 12 x 12 and 24 x 24-inch plates cut from No. 61 is approximately 760 and 840 grams, respectively.

2. The shock limit of 18 x 18-inch plates cut from No. 60 is approximately 870 grams. The only 18 x 18-inch plate of No. 61 material tested failed at 840 grams.

DISCUSSION OF RESULTS

Although the tensile properties of the two plates are essentially the same, the V-notch Charpy impact strength of plate No. 60 is consistently higher at 70, -40, and -320°F for specimens having the axis of the notch perpendicular to the rolling direction and parallel to the plate surface.

The difference in shock-limit and impact strength, may possibly be attributed to differences in heat treatment of the two plates, in the manufacturing practice if the two are from different heats, and, though less likely, in the chemical composition of the steel.

TABLE A-1 - DIRECT-EXPLOSION TESTS OF 12 x 12, 18 x 18, AND
24 x 24 x 1-INCH LOW-ALLOY Ni-Cr STEEL PLATE

(Detonation Velocity of Explosive Charge: 3512 mps)

Plate No.	Sheet No.	Plate Size in.	Weight of Charge gm	Dish mm	Fracture	Shock Limit gm	Dish at Shock Limit mm
S31	61	12 x 12 x 1	1200	--	Yes	760	83
32	"	"	1200	--	Yes		
36	"	"	900	--	Yes		
38	"	"	800	92	Yes		
43	"	"	760	83	No		
44	"	"	780	84	Yes		
45	"	"	780	84	Yes		
46	"	"	760	82	No		
S33	60	18 x 18 x 1	1000	108	Yes	870	80
34	"	"	900	81	Yes		
35	"	"	870	80	No		
37	"	"	890	81	No		
39	"	"	890	106	Yes		
40	"	"	880	108	Yes		
41	"	"	860	82	Yes		
42	61	"	840	88	Yes		
S47	60	24 x 24 x 1	920	76	Yes	840	72
48	61	"	880	83	Yes		
49	"	"	840	72	No		
50	"	"	860	71	Yes		
51	"	"	860	77	Yes		
52	"	"	840	71	Yes		
53	60	"	890	74	Yes		
54	"	"	860	82	Yes		

APPENDIX B

DETERMINATION OF DETONATION VELOCITY OF EXPLOSIVES*

The detonation velocity of an explosive powder is determined in the following way. In Fig. B-1, ABS represents a carefully prepared "stick" of the explosive packed to a standard density. Attached to this "stick" are two three-meter lengths of Ensign-Bickford Primacord, DEF and D'E'F', the detonation velocity of which is reproducible and known. A lead plate is placed under each Primacord length approximately 40 to 50 centimeters beyond the mid-length. The lengths of Primacord are cut accurately and the distance from one of the ends to a reference point on the lead plate is also measured accurately.

The "stick" of explosive is detonated at A and the wave progresses from A to DD'. When D and D' are reached, the wave starts along the legs DEF and D'E'F' and also continues along ABC. As the Primacord and the explosive under test are quite different, the detonation speeds are different. When the wave travelling from A to B reaches FF' it starts up the legs F to E and F' to E'. There are now two waves travelling toward each other in each Primacord leg. The impact of these waves produces a sharp line or pip on the surface of the lead plate.

From the measured lengths of Primacord, the known position of lead plates relative to the lengths of this explosive, the distance from the pip to the reference line, the distance DF and the known velocity of the Primacord, the velocity of the unknown powder may be calculated.

* Muller, A.; Benz, W.G.; Snelling, W.A.; "Preliminary Investigation of the Shock Resistance and Mechanical Properties of 0.5-inch Cr-Mo-V Aircraft Armor", Progress Report No. 1, WAL Report No. 110/13-9, May 1948.

For illustration, only one leg DEF will be used, the other leg D'E'F' merely serves as a check. Assume the following values were obtained.

$$\begin{aligned} \text{DEF} &= 300 \text{ cm} \\ \text{DF} &= 40 \text{ cm} \\ \text{FR} &= 100 \text{ cm} \\ \text{RP} &= 20 \text{ cm} \\ \text{DEF} &= \therefore 300 - (100 \neq 20) \\ &= 180 \text{ cm} \end{aligned}$$

$$\begin{aligned} V_p &= 6000 \text{ m/s} & V_p &= \text{Det. Vel. of Primacord} \\ V_x &= \text{ " " " } & V_x &= \text{ " " " explosive under test} \end{aligned}$$

Let t_1 = time for wave to travel from D toward E to P
 t_2 = " " " " " " " D to F
 t_3 = " " " " " " " F past R to P

At the instant of impact of the two opposite waves in leg DEF

$$t_1 = t_2 \neq t_3$$

then

$$\frac{\text{DEF}}{V_p} = \frac{\text{DF}}{V_x} \neq \frac{\text{FRP}}{V_p} \quad \left(\frac{1}{1/t} = t \right)$$

$$\frac{180}{6000} = \frac{40}{V_x} \neq \frac{120}{6000}$$

$$\frac{40}{V_x} = \frac{60}{6000} = \frac{1}{100}$$

$$V_x = 4000 \text{ mps}$$

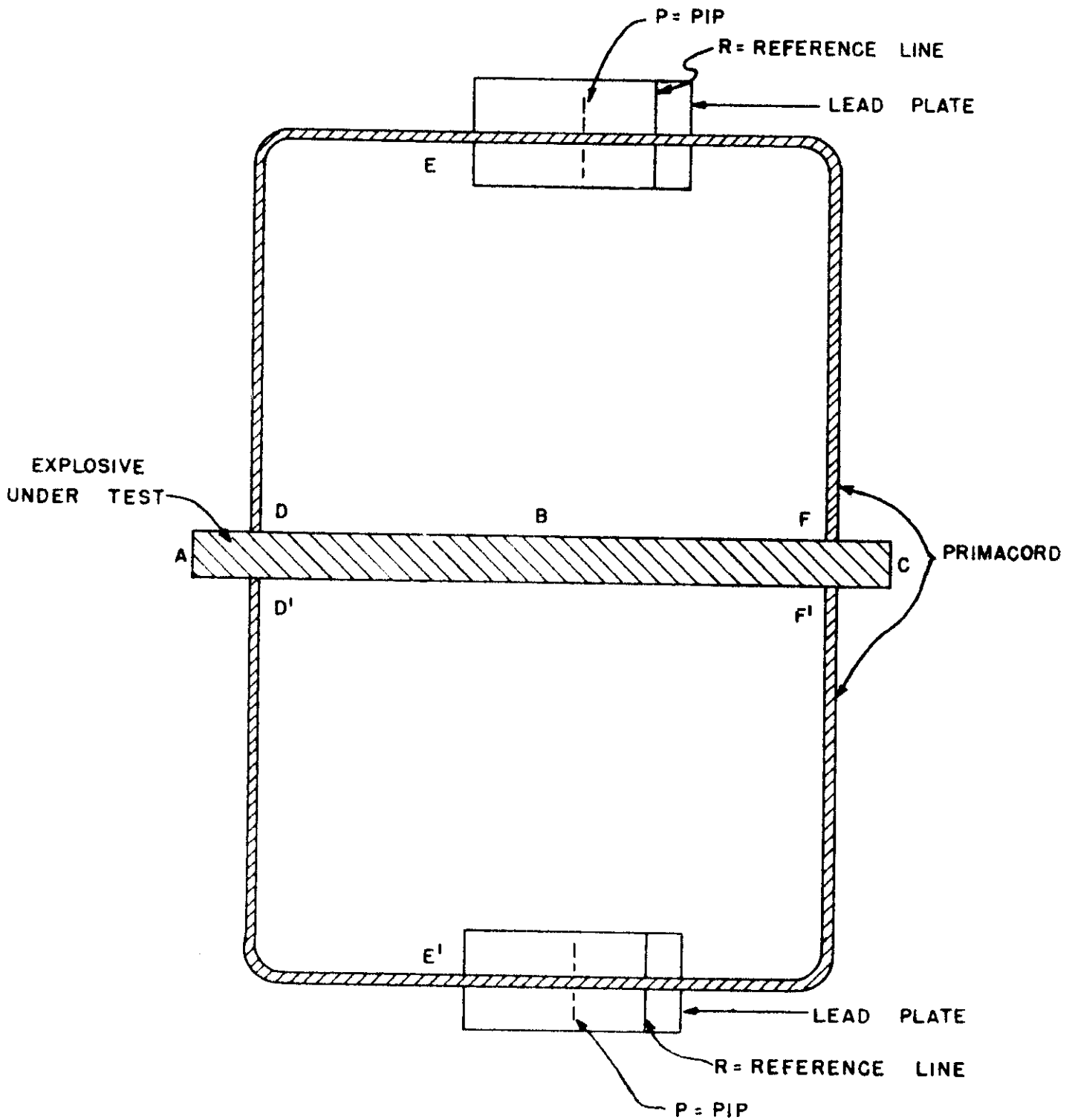


FIG. B-1 ARRANGEMENT FOR DETERMINING DETONATION VELOCITY

APPENDIX CCOMPARISON OF EFFICACY OF PLATEN QUENCHING AND BRINE
QUENCHING AFTER AUSTENITIZING OF Mn-Mo STEEL

The manganese-molybdenum steel submitted for direct-explosion tests was heat treated in the following way. 180 x 60 x 1-inch plates were heated in a continuous furnace for a total time of two hours, forty-five minutes in the temperature range of 1625 to 1650°F. Each plate was quenched using water-cooled platens. After quenching, each was tempered at 1215°F for four hours.

It is recognized that the shock resistance of a steel having a tempered martensite structure is superior to one having a tempered intermediate-transformation-product structure, tempered bainite, or free ferrite and carbide. The efficacy of platen quenching and brine quenching were compared in the following way.

Two three-inch diameter specimens of the plate were austenitized for 45 minutes at 1625°F, one was then placed between two water-cooled platens and the other was quenched by immersing in brine. Before tempering these pieces for four hours at 1215°F, a section was cut from each for hardness and microstructure studies. After tempering, another section was cut from each for further study.

Hardness measurements, notched-bar impact tests at 70 and -40°F, and microstructure examination were conducted. The results of these tests are listed below.

<u>Heat Treatment</u>	<u>Hardness,</u> <u>BHN</u>	<u>V-Notch Impact Strength,</u> <u>Ft-lb.</u>	
		<u>70°F</u>	<u>40°F</u>
As received (Platen Quench & Temper)	205	71.5	43.2
Platen Quench	200	--	--
Platen Quench and Temper	170	52.8	27.5
Brine Quench	374	--	--
Brine Quench and Temper	207	71.0	38.5

Examination of the microstructure of representative samples from sections heat treated as described above revealed:

1. Brine quenching by immersion produced a fully martensitic structure.
2. Tempering the brine-quenched sample at 1215°F for four hours produced a structure comprising uniformly dispersed fine carbide in a ferrite matrix.
3. Platen quenching this steel from 1625°F produced a structure comprising equiaxed ferrite, some acicular ferrite, and a fine carbide-ferrite aggregate indicating transformation was almost complete on cooling through the temperature range of 1200 - 1000°F.
4. Tempering the platen-quenched samples at 1215°F merely spheroidized the carbide particles. The carbides were not so uniformly dispersed as those in the tempered martensite structure and, therefore, the areas of free ferrite were large.
5. The commercially heat treated sample, as received, comprised a uniform dispersion of carbide in a ferrite matrix with a small amount of acicular ferrite. Apparently, this structure, before tempering, consisted of martensite and a small amount of acicular ferrite.

The results of this brief comparison of heat-treating procedures indicate:

- a. The laboratory platen quench was not as drastic, or complete, as that used by the steel producer as indicated by the low hardness of 200 BHN.

- b. The experimental platen-quench and temper treatment on this material produced a low hardness of 170 BHN with corresponding low impact values, 52.8 ft-lb at 70°F, and 27.5 at -40°F as compared to 205 BHN and impact values of 71.5 and 43.2 ft-lb at 70 and -40°F, respectively, for the commercially heat treated material.
- c. The hardness and impact strength of the brine-quenched and tempered material is essentially the same as that of the commercially treated material.

From these data, it is apparent that the platen-quenching and tempering treatment by the steel maker is as effective as brine quenching, but, probably not as consistent as might be, for differences in microstructure of pieces purportedly heat treated the same have been described earlier. It is entirely feasible that differences such as were observed in the microstructure of the commercially heat-treated steel may account for some of the anomalous results encountered in the direct-explosion test.

PART II

THEORETICAL INVESTIGATION OF THE FRACTURE OF
STEEL PLATES UNDER EXPLOSIVE LOADING

TABLE OF CONTENTS

	<u>Page</u>
I OBJECT	1
II ASSUMPTIONS AND PROCEDURE	1
III CONCLUSION	5
IV DISCUSSION AND RECOMMENDATION	6
V ANALYSIS	7
VI EXAMPLES	17
VII ACKNOWLEDGMENT	20
VIII BIBLIOGRAPHY	21

FIGURES FOLLOW BIBLIOGRAPHY

I. OBJECT

The object of this study was to investigate theoretically the state of stress existing in a plate which is subjected to an explosive load abutting the plate as shown in Fig. 1. The details of this particular test may be found in a previous report¹. Briefly, a standard charge of known velocity of detonation and known mass is placed against a plate which rests on a standardized base. Either the velocity of detonation or the mass of the charge is varied until the plate just shows signs of cracking on the side away from the charge. It is anticipated that the test will eventually be so standardized that it will be possible to separate materials according to their resistance to withstand shock loading. At present, there is no static test which can be substituted for a dynamic test to evaluate shock resistance.

If it were possible to obtain any theoretical knowledge of the state of stress existing in the plate during this test, even though it were approximate, such information might be of value in: interpreting the test, reducing the number of tests necessary, showing the explicit dependence of the parameters involved, and pointing the way for future rational experimentation.

An exact solution to the problem is not feasible at the present time since it is necessary to first ascertain what variables should be observed and, if possible, measured to aid in the extensions of the theoretical analysis.

II. ASSUMPTIONS AND PROCEDURE

The following are the principal assumptions made in the present approximate treatment:

1. References listed in bibliography, page 21.

1. The action of the explosive loading on the plate may be divided into two principal stages:
 - a. The propagation of elastic, plastic and release waves into the plate and their reflections and interactions, before the geometry of the plate changes, (before the plate bulges).
 - b. The plastic deformation of the plate in the large, that is, the dishing out of the plate and its changing geometry.

Only la. above of these cases is considered in this report. The possibility of fracture (cracking or spalling) in stage la is considered in detail.

It is further assumed that:

2. The impact and subsequent effects are plane in character and that waves which radiate outward are not reflected back into the region near the center of the plate in the interval of time prior to bulging. In effect an infinite plate is assumed.
3. Very little is known about the properties of materials under high rates of loading; in tests, such as these, the strain rates are assumed to be of the order of 10^6 per second. Neither stress-strain curves nor yield values have been accurately reported for such speeds.
4. Obviously, for a theoretical solution, it is necessary to establish a relation between stress and strain; therefore, it has been assumed that the true stress-strain curve consists of two straight lines as in Fig. 2. As it turns out, the exact value of the yield point is not critical for the results are not sensitive to yield point values at the high rates of loading so these values, therefore, may be estimated in some manner or simply assumed. A method for finding the slope of the straight line from the

yield point defining the region of plastic strain is presented in detail below,

5. A criterion for fracture is also necessary. This presents a grave difficulty because:
 - a. No such measure of fracture has proved satisfactory in all cases at ordinary rates of loading and
 - b. It is necessary to extrapolate to the high rates of loading from ordinary conditions.

Some time ago a criterion for fracture based on energy considerations was developed which postulated that fracture occurred when the energy density at the critical point in the body reached a certain value². One of the objects was to calculate the critical energy density for fracture. The postulate of a critical energy density will be retained here and fracture will be assumed to occur when the energy density (energy per unit volume) reaches the value given in the ordinary tensile test, as measured by the area under the true stress-strain curve for the test conducted at a low rate of loading.

There is some evidence to support the view that this procedure is at least approximately correct³. The stress-strain curve is assumed to comprise two straight lines as mentioned before and the slope of the plastic portion is obtained from an independent calculation of the velocity of the plastic wave and its relation to the slope of the stress-strain curve. Knowing the area under the curve at which fracture takes place, estimating the yield point, and calculating indirectly the slope of the straight line portion of the curve, it is possible to calculate the stress at fracture. This calculated stress is used as the criterion for fracture.

The procedure adopted is first to assume that the plate is hit by an infinite mass of gas of known velocity, the actual mass of gas being corrected

for afterwards. The velocity of the elastic wave which is first set up and the velocity of the plastic wave which follows can be calculated^{4,5}. The elastic wave is followed by a release wave which travels at the velocity of the elastic wave. It is further assumed that fracture takes place along the plastic wave front after it has been intersected by the release wave. A simplified dynamic analysis along lines developed by G. I. Taylor⁵ is given which relates stress to velocity of impact.

III. CONCLUSION

An approximate relation of the form

$$\frac{\sigma}{\rho} \ln \frac{L_1}{y} = 2V_0 C_p - V_0^2$$

has been developed where: σ is the tensile stress developed in the thickness direction of the plate

ρ is the density of the plate

L_1 is the original thickness of the plate

y is the thickness of the spalled part

V_0 is the uncorrected velocity of the impact

and C_p is the speed of the plastic wave.

From this relationship it is possible to determine whether or not a plate will fracture under a given charge of explosive and a given velocity of detonation. The velocity V_0 must be corrected approximately to V , where

$$V = \left(1 - \frac{M_2}{M_1} \right) V_0$$

M_1 being the mass of the explosive charge

M_2 an effective mass of steel plate

V_0 the velocity calculated by the preceding formula

and V is the actual velocity of detonation

This approximate formula gives a maximum stress when the velocity V_0 is equal to C_p . Actually, it is assumed that fracture always takes place when the velocity of the explosion is equal to the velocity of sound in the material. Since the velocity of both the plastic and elastic waves are close in value, the result obtained seems fairly reasonable.

IV. DISCUSSION AND RECOMMENDATION

The problem of finding the state of stress in a bar or wire when one end of the specimen has been subjected to an impact of known velocity has been worked out quite completely both graphically and numerically in a series of investigations conducted during the war^{4,7,8,9}. This work assumes that the static stress-strain curve continues to hold, or at most is raised twenty-five or thirty percent by dynamic loading, an assumption which is not unreasonable for comparatively low rates of loading but not justified in the present problem. This work also assumes a one-dimensional state of stress and strain and known initial conditions. To apply the methods to the explosive loading problem requires a knowledge of the pressure built up on the face of the plate by the explosion as a function of time. It also requires the assumption that the plate remains plane; that is, no changes in the geometry of the structure occur while the method of waves or characteristics is being applied. It is also necessary to assume an infinite plate in lateral dimensions so that there is no interference from surface waves reflected from the edges of the plate. All this can be done, but the important missing data are pressure as a function of time and stress-strain characteristic of the plate at the high rate of loading. Without this information the solution is not too accurate. An effort should, therefore, be made to obtain these data. Concurrently, the importance of the first time interval during which waves are being transmitted, reflected and are interacting, before the plate starts to bulge, should be investigated. Fractures which result from large deformations during bulging might well be examined by static methods.

Until the aforementioned basic data are obtained, it does not seem feasible to continue this theoretical analysis.

V. ANALYSIS

Figure 1 represents a section of plate in the thickness direction under explosive impact. The original thickness of this plate is L_1 and at the instant shown it is Z . Impact has taken place and first an elastic wave with speed C has advanced to the right as a compression wave. This is followed by a plastic wave, also compression, at a speed C_p and at the instant shown A-A is the plastic wave front.

Figure 2 shows a schematic representation of the idealized stress-strain curve for the material. OA is the elastic part of the curve, and AB the plastic region. It has been shown that the velocity of the stress wave in the elastic part is given by

$$C = \sqrt{\frac{E}{\rho}} \quad (1)$$

where E is the modulus of elasticity and ρ is the density. In the plastic region the velocity of the stress wave is given by⁷

$$C_p = \sqrt{\frac{1}{\rho} \left(\frac{d\sigma}{d\varepsilon} \right)} \quad (2)$$

which in our case reduces to

$$C_p = \sqrt{\frac{E_p}{\rho}} \quad (3)$$

E_p being the slope of AB

If the loading is not carried to fracture but is released at some point A', load is released along A'O' which has approximately the same slope as the elastic line OA. Later it is shown that this gives rise to a release wave having approximately the velocity of the initial elastic wave.

The above expressions for C and C_p are valid in the case of a bar or

wire with boundaries free to contract or expand as the case may be. If, as in the case of a plate, there are lateral restraints, these expressions must be modified⁵. When the wave is plane as assumed, equation (1) becomes

$$C = \left[\frac{3K}{\rho} \left(\frac{1-\nu}{1+\nu} \right) \right]^{\frac{1}{2}} \quad (4)$$

where C and ρ have the same meanings as before

and K is the bulk modulus

and ν is Poisson's Ratio

For steel the value of C is approximately 240,000 in/sec and this value will be used in what follows.

When the material is in the plastic state, $\nu = \frac{1}{2}$ and equation (4) becomes

$$C_p = \sqrt{\frac{K}{\rho}} \quad (5)$$

K may be estimated in various ways^{4,5}. Using a suitable value for K , calculation of C_p , according to the method of Koehler and Seitz, results in a value of 208,000 in/sec. Using the procedure of Pack, Evans, and James⁵ results in approximately the same value for C_p .

Referring to Fig. 3, which shows a cross section of the plate, the initial elastic wave is shown to start from t_0 and from the compression face. When the elastic wave has reached the opposite side of the plate, it is reflected as a tension wave and interacts with the oncoming plastic wave which follows the elastic wave and travels at a slower speed. This results in a series of reflections and transmissions. In the meantime the gas pressure has fallen off and, at time t_1 , a release wave having the same velocity as the elastic wave is set up in the material. This in turn may interact with the preceding waves.

This process is pictured in Figs. 3 and 4 which show two possibilities; (1) the plastic wave reaches the opposite side of the plate before being caught by the release wave, Fig. 3, and (2) the release wave reaches the plastic wave, Fig. 4. Which phenomenon occurs depends on the thickness of the plate and the time of duration of the applied pressure pulse, designated by T .

It should be noted that Figs. 3 and 4 are simplified by the assumption that the stress-strain curve comprises two straight line portions. Otherwise each reflection of a wave would give rise to a set of characteristics instead of a single line. Examples may be found in the literature^{8,9}.

Koehler and Seitz⁴ classify plates as "thick" if the release wave overtakes the plastic wave before any of the reflected waves can get back to the plastic front; plates are classified "thin" if the release wave does not overtake the plastic front before the release wave reaches the free surface. There are, of course, intermediate cases.

The classification is important because it seems likely that spalling will occur only in the case of the "thick" plate. This "thickness" may be obtained either by having a plate of considerable depth or by making T , the duration of the peak pressure, very small. In other words, applying a short, sharp pulse to the plate increases the tendency to spall.

This does not completely define the problem of fracture before a change in geometry of the plate can take place because if an explosive having a detonation velocity equal to the velocity of sound in the material is detonated against a plate, fracture should occur regardless of the duration of impact. An explanation for this follows:¹⁰

The vibrational frequency of an atom in a metal is about 10^{13} per second while the distance between equilibrium positions is of the order of 10^{-8} cm. If one surface is pulled over an immediately

adjacent surface at the rate of one centimeter per second, the time spent in each potential well (minimum) is about 10^{-8} seconds. During this time the atom vibrates about 10^{15} times, thereby enabling it to dissipate as heat the activation energy necessary to propagate the slip or fracture. Thus activation energy must be furnished anew for each jump in the process. If slippage is rapid and the atom makes relatively few vibrations in each minimum energy position little of the activation energy is dissipated and the system, after having been brought over the first potential barrier, can coast over the tops of the potential barriers thereby providing an effective mechanism for fracture propagation.

It is assumed that fracture, if it takes place at all will occur just ahead of the advancing wave front and probably only if the release wave intersects the plastic wave. Interest centers only on the type of fracture that takes place before the plate bulges, i.e., before any waves radiating laterally are reflected from the edges and thus further complicating the picture.

Following the analogous work of G. I. Taylor⁶, the elastic region of Fig. 1 is taken as a free body. Using the sign convention designated in Fig. 5, the equation of motion is written for the piece of the plate. Unit area, A, in the XY plane is assumed and the thickness of the plate effected by elastic action is designated as Y . There results

$$-\sigma = \rho Y \frac{d^2 Z}{dt^2} \quad (6)$$

Assuming that Y and Z are related through

$$Y = Z - C_p t \quad (7)$$

we obtain

$$\frac{d\gamma}{dt} = \frac{dz}{dt} - c_p \quad (8)$$

and

$$\frac{d^2\gamma}{dt^2} = \frac{d^2z}{dt^2} \quad (9)$$

Thus equation (6) may be written

$$-\frac{\sigma}{\rho} = \int \frac{d^2\gamma}{dt^2} \quad (10)$$

Where σ is the stress just behind the elastic region and ρ is the density

Let

$$u = \frac{d\gamma}{dt} \quad (11)$$

so

$$\frac{d^2\gamma}{dt^2} = \frac{d\gamma}{dt} \cdot \frac{du}{d\gamma} = \frac{u du}{d\gamma} \quad (12)$$

and equation (10) becomes

$$-\frac{\sigma}{\rho} = \int u \frac{du}{d\gamma} \quad (13)$$

The variables may now be separated and integrated, yielding

$$-\frac{\sigma}{\rho} \int_{L_1}^{\gamma} \frac{d\gamma}{\gamma} = \int_{(w_0 + c_p)}^u u du \quad (14)$$

The limits are determined from the fact that when $t = 0$, $\gamma = L_1$ and

$$\frac{dz}{dt} = -\left(\frac{dz}{dt}\right)_t = 0$$

which is designated by w_0 the initial velocity of impact.

The sign is in accordance with the sign indicated in Fig. 5. The same result would occur if it had been assumed that the gas is at rest and

the section of the plate strikes the gas with initial velocity $|w_0|$.

Since $\frac{dz}{dt} = \frac{dJ}{dt} - C_p$ the lower limit on the right hand side of

equation (14) becomes $-(w_0 - C_p)$

Integrating equation (14) leads to

$$-\frac{2\sigma}{\rho} \ln \frac{J}{L_1} = u^2 - (w_0 + C_p)^2 \quad (15)$$

or

$$\frac{2\sigma}{\rho} \ln \frac{J}{L_1} = \left(\frac{dJ}{dt}\right)^2 - (w_0 + C_p)^2 \quad (16)$$

Suppose fracture takes place when $J = J_1$ and at that instant

$\sigma = \sigma_f$ also at this instant $\frac{dz}{dt} = 0$ or $\frac{dJ}{dt} = C_p$

Actually with the coordinate system chosen, the initial w_0 is negative, therefore $|w_0| = V_0$

Equation (16) becomes

$$\frac{2\sigma_f}{\rho} = \ln \frac{L_1}{J_1} = C_p^2 - (C_p - V_0)^2 \quad (17)$$

or

$$\frac{2\sigma_f}{\rho} = \ln \frac{L_1}{J_1} = 2V_0 C_p - V_0^2 \quad (18)$$

If V_0 and C_p are known, the right hand side of equation (18) is determined and

if J_1 is known, T may be found. If $\sigma \geq \sigma_f$ fracture takes place at the point

$J = J_1$ under the assumption that fracture takes place within a few reflections of the elastic wave and before the plate can bulge.

Two procedures are available to determine J_1 . First, the criterion that the crack is not to exceed a certain depth may be used. As an illustration,

suppose the depth of a crack which is 1/16" long is determined; say it is .01 inch. Then in a plate of 0.5-inch thickness, $\frac{L}{\gamma} = 50$ and $\ln 50 = 4$. The results are not particularly sensitive to changes in γ and in the numerical examples to follow, it is assumed that

$$\ln \frac{L_1}{\gamma} \approx 5 \quad (19)$$

Another way of estimating the distance J_1 is through an analysis of the time required for the waves to reach various places in the plate. The reason for this analysis of the time is to get the approximate expression for J_1 from the assumption that J_1 will be at some one of the points B, D, F, etc. on Fig. 6. This leaves an element of uncertainty, nevertheless it may be decided within limits, whether or not the plate will crack under the applied shock.

The equation of line AB, Figure 6, is

$$Z - L_1 = -C \left(t - \frac{L_1}{C} \right)$$

or

$$Z = -Ct + 2L_1 \quad (20)$$

To find the coordinates of point B, find the intersection of AB with line OB which has the equation

$$Z = C_p t \quad (21)$$

Solving equations (20) and (21) simultaneously results in

$$\begin{aligned} t_B &= \frac{2L_1}{C + C_p} \\ Z_B &= \frac{2L_1 C_p}{C + C_p} \end{aligned} \quad (22)$$

Therefore

$$L_1 - Z_B = J_B = \frac{C - C_p}{C + C_p} \cdot L_1 \quad (23)$$

Similarly, the coordinates of D, F, etc. may be found, also may be found the distances

$$\begin{aligned} Y_D &= L_1 - Z_D = L_1 \left(\frac{C - C_p}{C + C_p} \right)^2 \\ Y_F &= L_1 - Z_F = L_1 \left(\frac{C - C_p}{C + C_p} \right)^3 \\ &\text{etc.} \end{aligned} \quad (24)$$

In general

$$\ln \frac{L_1}{Y_1} = \ln \left(\frac{C + C_p}{C - C_p} \right)^n$$

or

$$\ln \frac{L_1}{Y_1} = n \ln \left(\frac{C + C_p}{C - C_p} \right) \quad (25)$$

where n is the number of reflections taking place before fracture.

Using equation (25), our previous equation (18) becomes

$$\frac{2 \sigma_f^n}{\rho} = \ln \frac{C + C_p}{C - C_p} = 2 V_0 C_p - V_0^2 \quad (26)$$

However, in this work,

$$\ln \frac{C + C_p}{C - C_p} \approx 2.51 \quad (27)$$

Thus the following may be written

$$\frac{5 \sigma_f^n}{\rho} = 2 V_0 C_p - V_0^2 \quad (28)$$

and this last equation is seen to agree with equation (19) if n is taken as 2.

It should be remembered that the V_0 is the initial velocity of the plate taken as if the plate had struck a gas of infinite mass which was at rest and remained at rest. An approximate correction must be resorted to.

Assuming a straight forward impact in which the coefficient of restitution between gas and plate is zero and using the conservation of momentum principle we obtain, see Fig. 7

$$m_1 V_1 + m_2 V_2 = m_1 V_1' + m_2 V_2' \quad (29)$$

but $V_2 = 0$ (30)

and $V_1' = V_2'$

Thus $m_1 V_1 = (m_1 + m_2)V$ (31)

where $V_1' = V_2' = V$

V corresponds to the quantity v_0 in equation (18) or (28), and v_1 is the actual speed of detonation of the explosion. Thus when this expression is solved for v_0 it is necessary to obtain V_1 from

$$V_1 = \left(1 + \frac{m_2}{m_1}\right)V \quad (32)$$

or $V_1 = \left(1 + \frac{m_2}{m_1}\right)V_0$ (33)

The problem now arises as to what value σ_f assumes at fracture. Unfortunately, it is impossible to use a maximum stress criterion for fracture. Even if such a criterion were known to be valid and the critical value at ordinary rates of loading were known, the problem of extrapolating to very high rates of loading would still remain. In order to handle the problem with the available knowledge, it is assumed:

1. The area under the true stress-strain curve remains constant to fracture regardless of the manner in which the fracture is brought about.
2. The stress-strain curve may be approximated to by two straight lines.
3. The strain energy of the elastic portion may be neglected; this amounts to neglecting the area under the elastic part of the curve, though for refinement of the results, it would be possible to consider this portion.

As may be seen from Fig. 8, calling A the area under the stress-strain curve,

$$A = \frac{\Sigma_f'}{2} (\sigma_p' - \sigma_f') \quad (34)$$

Since

$$\Sigma_f' = \frac{\sigma_f'^2 - \sigma_p'^2}{p} \quad (35)$$

this may also be expressed

$$A = \frac{\sigma_f'^2 - \sigma_p'^2}{2p} \quad (36)$$

All the information needed for the determination of A in equation (36) may be obtained from a simple tensile test at ordinary rates of loading. If the rate of loading is changed and the new stress-strain curve is assumed to have the shape shown in Fig. 9, A is determined, but σ_p and the slope p are needed in order to find σ_f' . This is done as follows: the new yield stress σ_p is undoubtedly higher than σ_p' but its new value, as will be evident, is not critical. In other words σ_p is unessential. The change in the slope of the curve from p' to p may be obtained from the independent calculation of the speed of sound in the plastic state. As noted previously,

$$C_p = \sqrt{\frac{1}{p} \frac{d\sigma}{d\varepsilon}} = \sqrt{\frac{p}{p'}} \quad (37)$$

Thus

$$p = p' C_p^2 \quad (38)$$

This last equation gives a value of p which corresponds to an elevation of the flow curve due to the increased rate of loading.

In this work $C_p = 208,000$ inches/second and $\rho = 7.2 \times 10^{-4}$ in the units of $\frac{lb/in^3}{in/sec^2}$ or $\frac{lb-sec^2}{in^4}$

$$\text{Thus } p = 29.9 \times 10^6 \text{ lb/in}^2 \quad (39)$$

and this value will be used in succeeding examples.

Examples

1. In a Jessop aircraft armor tested at room temperature and at ordinary rates of loading, it is estimated that

$$\begin{aligned} \sigma_f &= 234,000 \text{ lbs/in}^2 \\ \sigma_p &= 162,000 \text{ lbs/in}^2 \\ \text{and } \Sigma_p &= 0.432 \end{aligned}$$

$$\text{Thus } A = \frac{0.432}{2} \times 396,000 = 8.55 \times 10^4$$

$$8.55 \times 10^4 = \frac{\sigma_f^2 - \sigma_p^2}{2 \times 29.9 \times 10^6}$$

$$\sigma_f^2 = 2 \times 29.9 \times 10^6 \times 8.55 \times 10^4 + \sigma_p^2$$

σ_p will be of the order of 2×10^5 and may be neglected.

$$\sigma_f = 10^5 \times 22.6 = 2.26 \times 10^6 \text{ psi}$$

Suppose now that the speed of impact is 150,000 in/sec, using equation (18)

$$\text{with } \ln \frac{L_1}{J_1} = 5,$$

$$\sigma_f = \frac{7.2 \times 10^4}{10} \cdot \left[2 \times 150,000 \times 208,000 - \frac{150,000^2}{10} \right]$$

$\sigma_f = 2.7 \times 10^6$ which is greater than the calculated fracture stress and it is concluded that such a speed would fracture the plate. This speed corresponds to the value of V and it should be related to v_1 through equation (33).

If the speed is 100,000 in/sec, in a similar manner

$$\sigma_f = 7.2 \times 10^{-5} \left[2 \times 100,000 \times 204,000 - \overline{100,000^2} \right]$$

$$\text{or } \sigma_f = 2.22 \times 10^6 \text{ psi}$$

and fracture does not occur.

The values, however, refer to the relative speed and should be corrected. However, it is a question how the ratio M_2/M_1 should be determined.

The actual weight of the charge can be used for M_1 and M_2 estimated by assuming that the thickness of steel which is given the initial velocity is about 1/10th the thickness of the plate. Taking the density of steel as 7.8 and considering a section of 7.5 cm diameter and $1/10 \times (1.27) = .127$ cm thick the weight is calculated to be 45 grams. If the charge is 400 grams,

$$V = \left(1 + \frac{45}{400} \right) 110,000 = 121,000 \text{ in/sec}$$

to fracture the plate, this is about 3040 meters/sec and represents the actual speed of detonation.

For a charge of 300 grams,

$$V = \left(1 + \frac{45}{300} \right) 110,000 = 127,000 \text{ in/sec}$$

or about 3200 meters/sec

The figure 1/10th of the thickness of the plate is an arbitrary one and may be adjusted.

2. Mn-Mo Steel

Yield Strength	~	85,200 psi
Fracture Load	~	12,900 lbs

Initial Diameter	0.503
Final Diameter	0.288
True Fracture Stress	198,000 psi

Calculation

Logarithmic Strain at Fracture

$$\Sigma = 2 \ln \frac{.503}{.288} = 2 \ln 1.75 = 1.12$$

$$A = \frac{1.12}{2} (198,000 + 85,200) = 158,000$$

$$158,000 = \frac{\sigma_f^2 - \sigma_p^2}{2 \times 29.2 \times 10^6}$$

$$\sigma_f^2 \approx (158,000) \cdot (2 \times 29.9) \cdot (10^6)$$

$$\sigma_f \approx 3.07 \times 10^6 \text{ psi}$$

$$\text{now } \sigma = 7.2 \times 10^{-5} (2 v_0 c_p - v_0^2)$$

using $c_p = 208,000$ in/sec

and $v_0 = 208,000$, the highest possible in this theory, it is seen that it is necessary to go at least up to the speed of the plastic wave in order to have fracture. Then

$$\underline{v} = \left(1 + \frac{M_2}{M_1} \right) \times 208,000 \text{ in/sec}$$

or probably, for a 400 gram charge

$$\underline{v} = 222,000 \text{ in/sec or about } 5500 \text{ meters/sec.}$$

VII. ACKNOWLEDGMENT

The author wishes to express his thanks to Dr. A. Muller and to Mr. W. G. Benz of the Air Reduction Laboratories for their kind help and encouragement in this project. He is particularly indebted to them for the preparation of the report.

VIII. BIBLIOGRAPHY

1. Muller, A.; Benz, W. G.; Snelling, W. A.: "Watertown Arsenal Laboratory Progress Report No. 110/13-9. Preliminary Investigation of the Shock Resistance and Mechanical Properties of 0.5-inch Cr - Mo - V Aircraft Armor." May, 1948, Restricted.
2. Saibel, E.: "A Thermodynamic Theory of the Fracture of Metals," AIME Technical Publication 2131 (1947).
3. Ljungberg, K.: "Constancy of Work Done in Fracture as Explanation for Fracture Caused by Fatigue and Other Loadings." Zeit V.D.I. Pamphlet #24 (1929).
4. Koehler, J. D. and Seitz, F.: "The Stress Waves Produced in a Plate by a Plane Pressure Pulse." NDRC Armor and Ordnance Report No. A-245 (OSRD No. 3230) (1944).
5. Pack, D. C., Evans, W. M.; James H. J.: "The Propagation of Shock Waves in Steel and Lead." Proc. Phys. Soc. 60 1-8, (1948).
6. Taylor, G. I.: "The Testing of Materials at High Rates of Loading." Journ. Inst. of Civil Eng. pp 486-519, (1946).
7. Karman, T.: "On the Propagation of Plastic Deformation in Solids." NDRC Report A-29 (OSRD No. 365) (1942).
8. Karman, T.; Bohlenblust, H. F.; Hyers, D. H.: "The Propagation of Plastic Waves in Tension Specimens of Finite Length." NDRC Report A-103, (1942).

9. Simpson, O. C.; Fireman, E. L.; Koehler, J. S.: "High Speed Compression Testing of Copper Crusher Cylinders and Spheres." NDRC Report No.A-25S (OSRD No. 3330) (1944).

10. Eyring, H.; Powell, R. E.: "Rheological Properties of Simple and Colloidal Systems." Colloid Chemistry, Vol. 5, p249; Edited by J. Alexander, Reinhold Publishing Co., New York (1944).

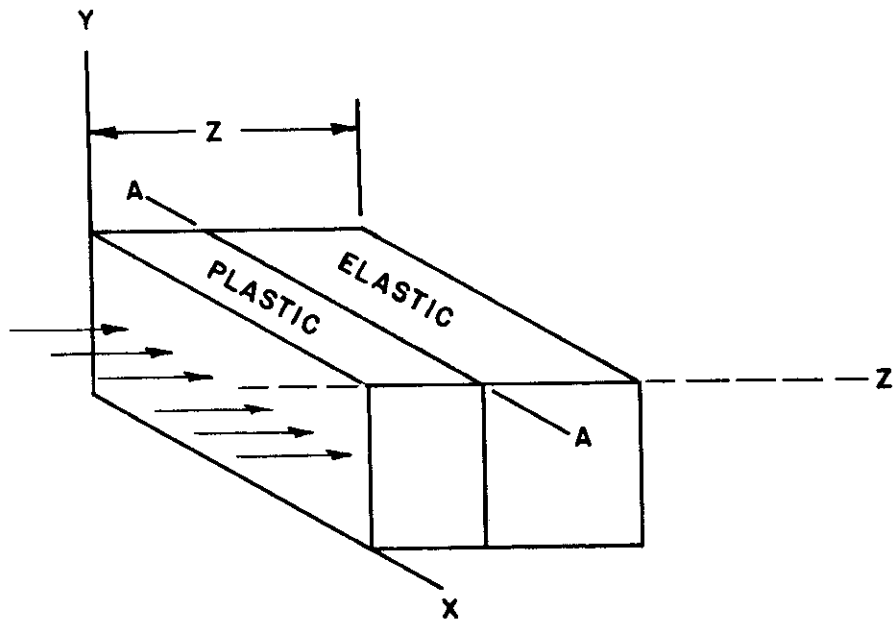


FIG. 1

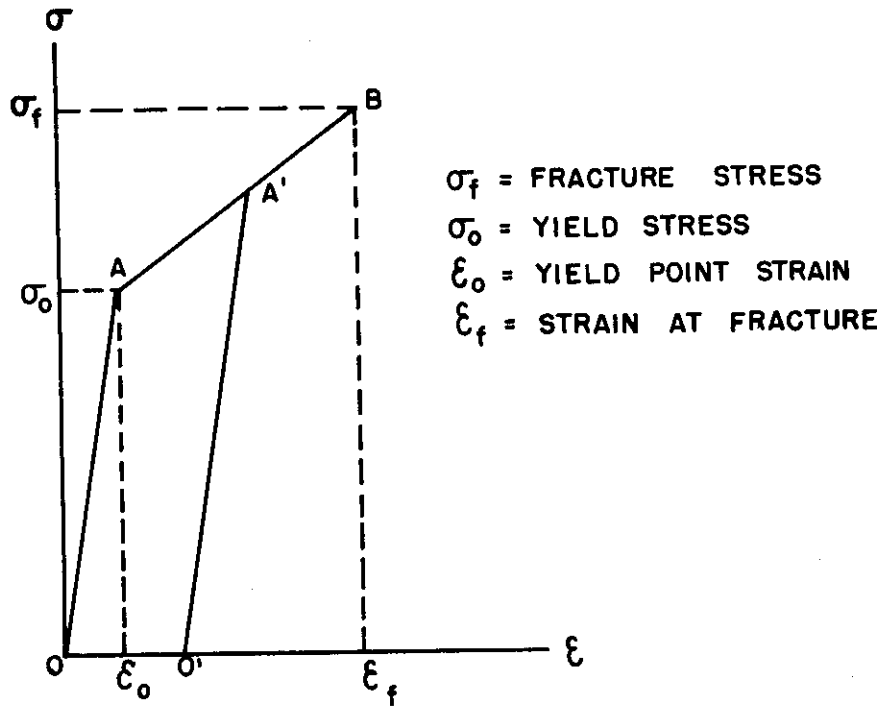


FIG. 2

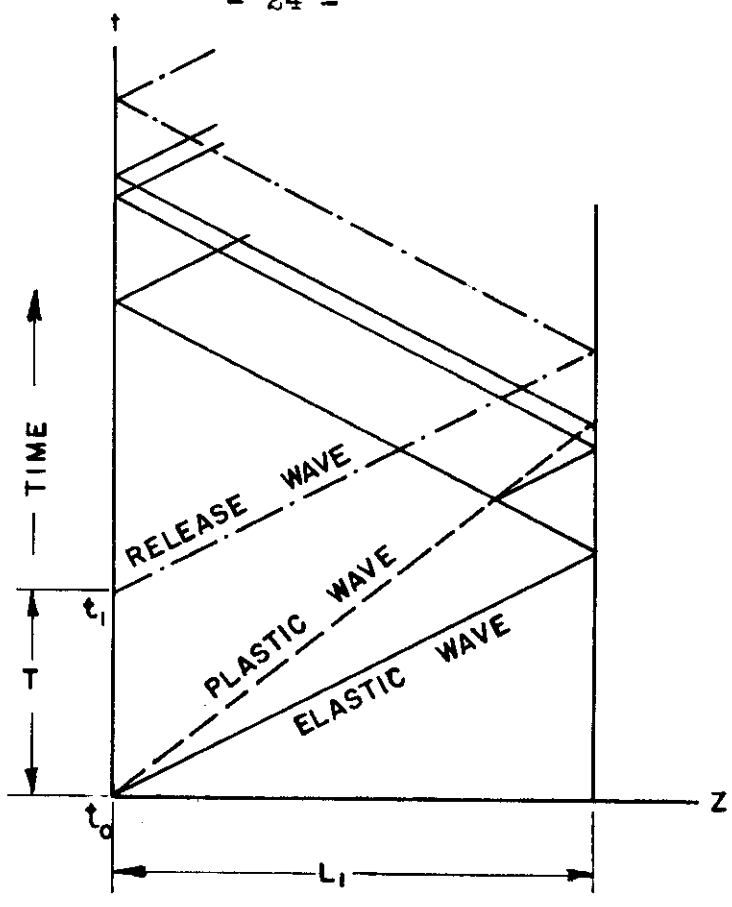


FIG. 3

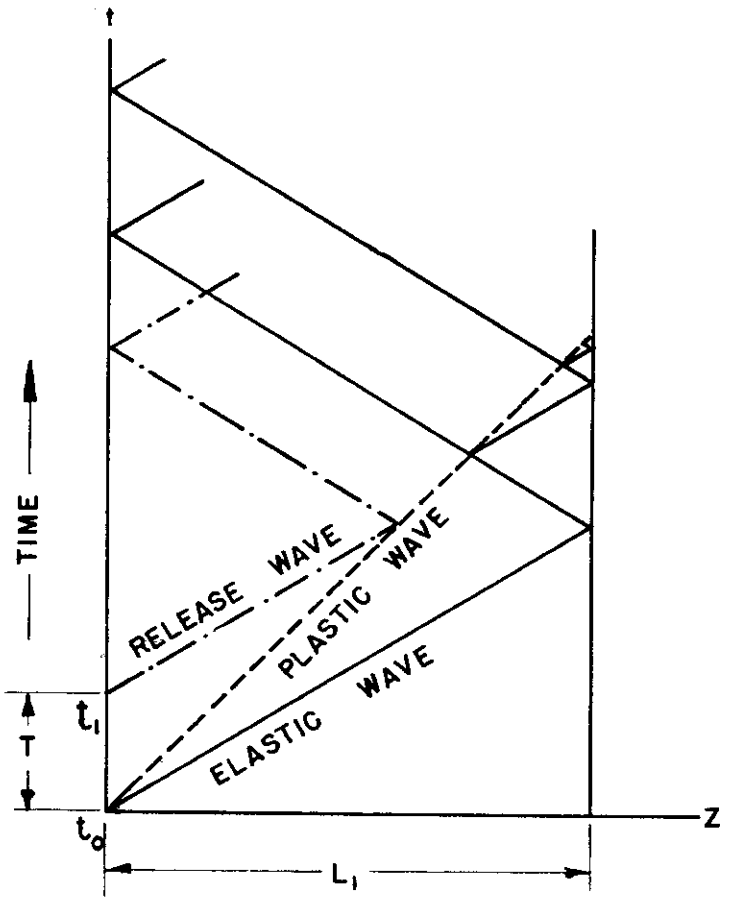


FIG. 4

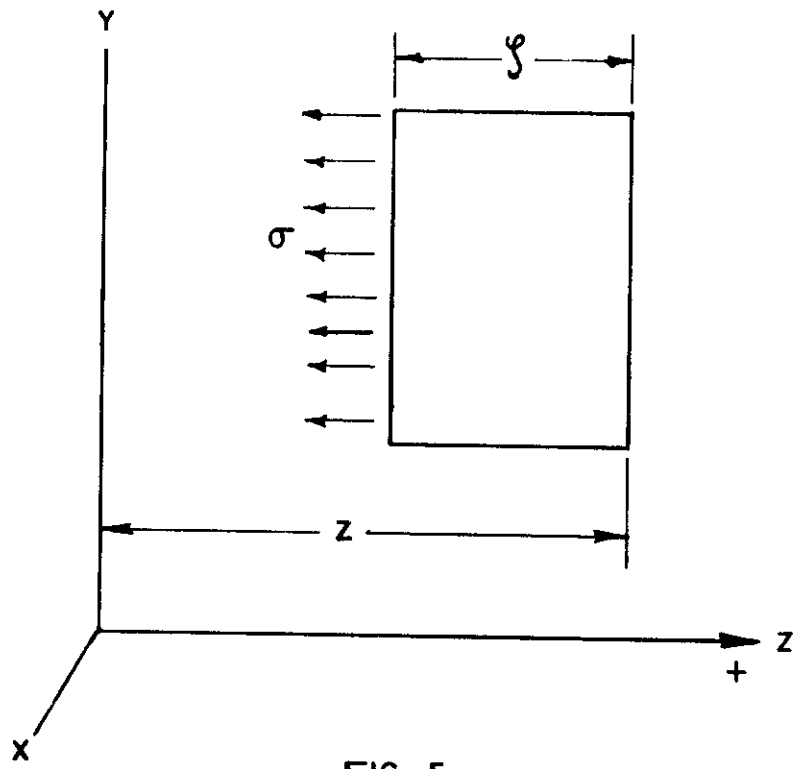


FIG. 5

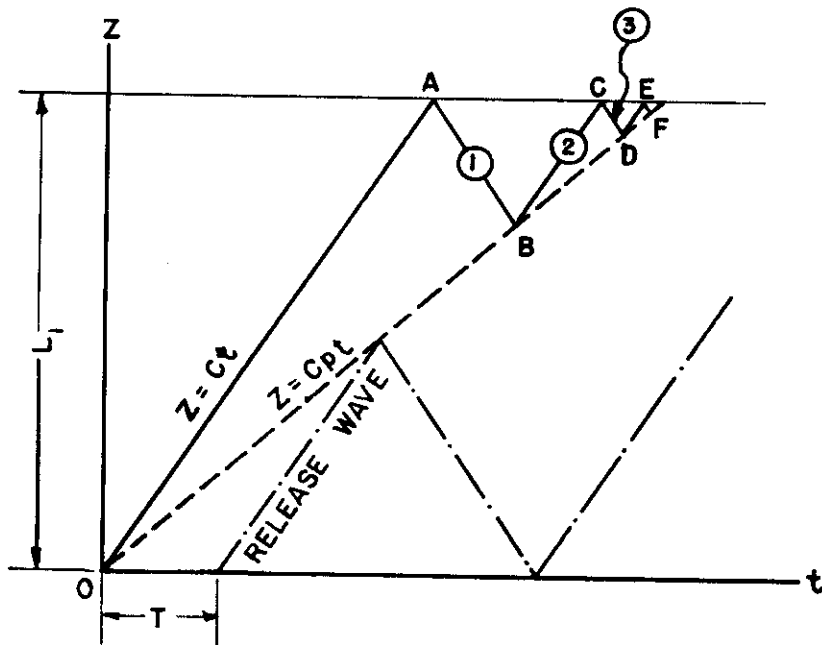


FIG. 6

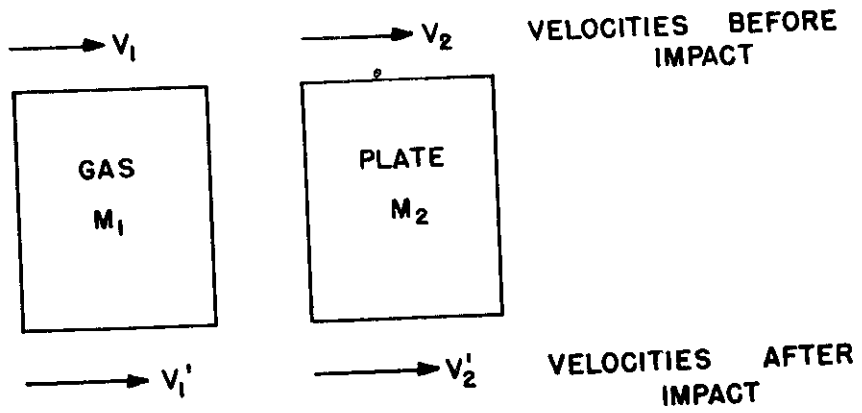


FIG. 7

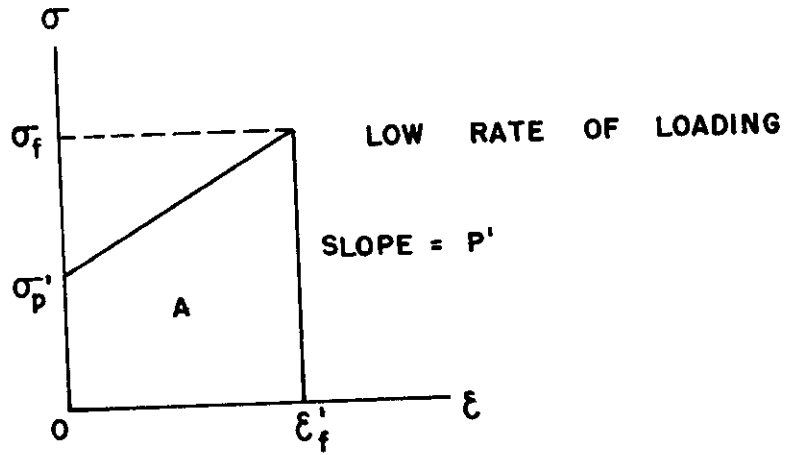


FIG. 8

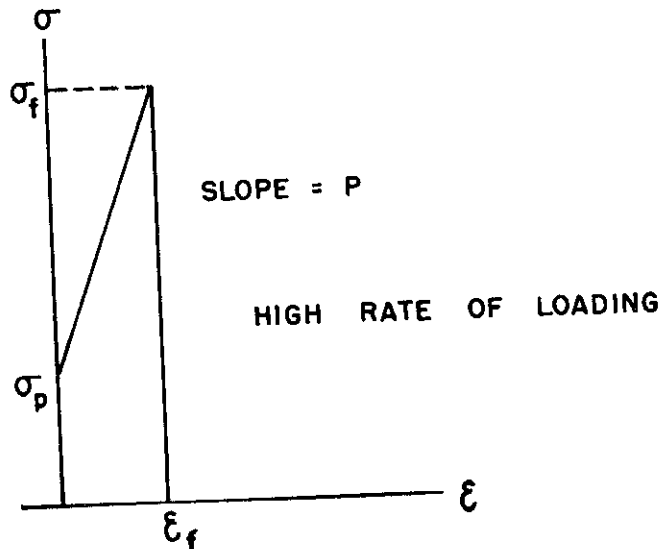


FIG. 9